Dept. of Math. Univ. of Oslo
Pure Mathematics No. 33
ISSN 0806–2439 October 2005

ON AN EXTENDED CLARIFIER-THICKENER MODEL WITH SINGULAR SOURCE AND SINK TERMS

R. BÜRGER[A], A. GARCÍA[A], K.H. KARLSEN[B], AND J.D. TOWERS[C]

Abstract. A well-studied one-dimensional model for the operation of clarifier-thickener units in engineering applications can be expressed as a conservation law with a flux that is discontinuous with respect to the spatial variable. This model also includes a singular feed source. In this paper, the clarifier-thickener model is extended by a singular sink through which material is extracted from the unit. A difficulty is that in contrast to the singular source, the sink term cannot be incorporated into the flux function; rather, the sink is represented by a new non-conservative transport term. The paper is concerned with the well-posedness analysis and numerical methods for the extended model. To simplify the analysis, a reduced problem is formulated, which contains the new sink term of the extended clarifier-thickener model, but not the source term and flux discontinuities that can be handled by existing methods. A definition of entropy solutions, based on Kružkov-type entropy functions and fluxes, is provided. Jump conditions are derived and uniqueness of the entropy solution is shown. Existence of an entropy solution is shown by proving convergence of a monotone difference scheme. Combining the present analysis for the reduced problem with previous results [Numer. Math. **97** (2004) 25–65] shows that the full extended clarifier-thickener model is well-posed. Two variants of the numerical scheme are introduced. Numerical examples illustrate that all three variants converge to the entropy solution, but introduce different amounts of numerical diffusion.

1. Introduction

In recent years there has been an increased interest in the well-posedness and numerical analysis of conservation laws with a discontinuous flux of the type

$$u_t + f\big(\boldsymbol{\gamma}(x), u\big)_x = 0, \quad x \in \mathbb{R}, \quad t > 0, \tag{1.1}$$

where the flux function depends on a vector $\boldsymbol{\gamma}(x)$ of parameters that are discontinuous functions of the spatial position x. Applications of (1.1) and its extensions to systems of conservation laws and strongly degenerate parabolic equations include two-phase flow in heterogeneous porous media [32, 53], traffic flow on highways with changing road surface conditions [6, 41], ion etching models [48], shape-from-shading problems [46], endovascular treatment [16], population balance models for ball wear in grinding mills [11], and clarifier-thickener models, which motivate the

Date: October 26, 2005.
Key words and phrases. Conservation law, discontinuous flux, source term, sink term, entropy solution, jump condition, numerical method.

[A]Departamento de Ingeniería Matemática, Facultad de Ciencias Físicas y Matemáticas, Universidad de Concepción, Casilla 160, Concepción, Chile. E-Mail: rburger@ing-mat.udec.cl, agarcia@ing-mat.udec.cl.
[B]Centre of Mathematics for Applications (CMA), University of Oslo, P.O. Box 1053, Blindern, N–0316 Oslo, Norway. E-Mail: kennethk@math.uio.no.
[C]MiraCosta College, 3333 Manchester Avenue, Cardiff-by-the-Sea, CA 92007-1516, USA. E-mail:john.towers@cox.net.

present paper. The basic difficulty is that the well-posedness and numerical analysis for this equation does not emerge in a straightforward fashion as a limit case of the well-established theory for conservation laws with a flux that depends smoothly on the spatial variable x. In fact, several extensions of the entropy solution concept due to Kružkov [38] to a flux that depends discontinuously on x have been proposed in recent years [1, 3, 29, 30, 33, 35, 36, 37, 40, 49, 51, 52]. Each of these concepts is supported by a convergence analysis of a suitable numerical scheme; the differences between them appear in different admissibility conditions for stationary jumps across the discontinuities of $\boldsymbol{\gamma}$ [8]. The choice of the right entropy solution concept for (1.1) depends on the regularizing viscous physical model involved. For clarifier-thickener models, the appropriate entropy solution concept emerges from taking the limit $\varepsilon \to 0$ of a simple viscous regularization εu_{xx} with a global diffusion constant $\varepsilon > 0$; see [12, 14] for details.

Important contributions to the analysis of and the construction of exact solutions for clarifier-thickener models were made by Diehl [18, 19, 20, 21, 22, 23], in which local-in-time existence and uniqueness results for problems with piecewise constant initial data are obtained [18, 19, 21], stationary solutions are completely classified [21, 23] and numerical solutions using a Godunov-type scheme are presented [19, 21, 22]. On the other hand, in a series of papers including [5, 7, 9, 10, 12, 13] the authors with collaborators developed an activity aiming at providing a rigorous ground of well-posedness and numerical analysis for clarifier-thickener models. The basic non-standard ingredient of all clarifier-thickener models studied so far is a singular feed source that produces diverging bulk flows in the unit, and eventually generates the discontinuous x-dependence of the flux. It is the purpose of this paper to present a new extended clarifier-thickener model that also includes a singular sink term, through which material may be extracted, and to show that the new model, which is not included as a special case in previous analyses, is well-posed and can be simulated by a convergent numerical scheme.

Clarifier-thickener units are widely used in chemical engineering, wastewater treatment, mineral processing and other applications to separate a suspension of finely divided solid particles dispersed in a viscous fluid into its solid and liquid components. The basic clarifier-thickener model can be derived from the scalar conservation law

$$u_t + b(u)_x = 0, \quad x \in [0, L], \quad t > 0, \tag{1.2}$$

$$u(x, 0) = u_0(x), \quad x \in [0, L], \tag{1.3}$$

of the kinematic sedimentation model [15, 39], which describes the settling of a suspension of initial concentration $u_0(x)$ in a settling vessel of height L. Here, u is the sought concentration as a function of depth x and time t, and $b(u)$ is the hindered settling function or batch flux density function, which is a material-dependent function. A typical example is the Richardson-Zaki [47] type function

$$b(u) = \begin{cases} v_\infty u(1-u)^n & \text{for } u \in [0, u_{\max}], \\ 0 & \text{otherwise,} \end{cases} \qquad n > 1, \quad v_\infty > 0, \tag{1.4}$$

where v_∞ is the settling velocity of a single particle in an unbounded medium.

Suppose now that instead of letting the suspension settle in a closed vessel, we pump it into a vertical tube that is filled with water at a feed level $x = 0$, and that part of the mixture flows upwards (i.e., in the direction of negative x) at velocity

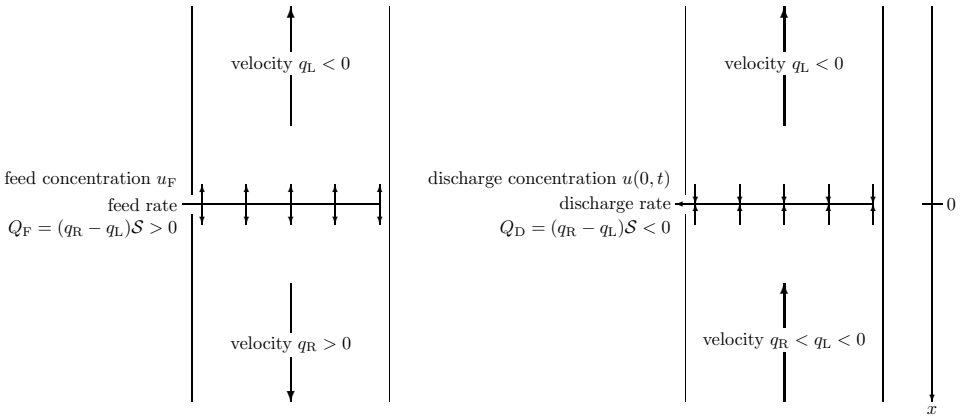

FIGURE 1. Basic flow variables for a singular source term (left) and a singular sink term (right).

$q_L < 0$, while the remainder flows downwards at velocity $q_R > 0$, as in the left diagram of Figure 1. Consequently, if $\mathcal{S}$ is the cross-sectional area of the tube, then $Q_F = (q_R - q_L)\mathcal{S}$. Assuming for a moment that we inject only clear water at $x = 0$, we obtain (instead of (1.2)) the conservation law with discontinuous flux

$$u_t + \big(q(x)u + b(u)\big)_x = 0, \quad q(x) := \begin{cases} q_L < 0 & \text{for } x < 0, \\ q_R > 0 & \text{for } x > 0. \end{cases} \tag{1.5}$$

Now let us inject feed suspension of a given concentration u_F (instead of water) at a volume rate Q_F. Since the feed source is concentrated at $x = 0$, we need to add the singular source term $\delta(x)(q_R - q_L)u_F$ to the right-hand side of the PDE in (1.5), obtaining

$$u_t + \big(q(x)u + b(u)\big)_x = \delta(x)(q_R - q_L)u_F. \tag{1.6}$$

However, using the Heaviside function $H(x)$, we may formally write $\delta(x)(q_R - q_L)u_F = (H(x)(q_R - q_L)u_F)_x$. Then (1.6) assumes the form

$$u_t + \big(q(x)u + b(u)\big)_x = \big(H(x)(q_R - q_L)u_F\big)_x$$

or equivalently,

$$u_t + \Big(q(x)u + b(u) - \big(H(x)(q_R - q_L)u_F\big)\Big)_x = 0, \tag{1.7}$$

so that the singular source is expressed as a discontinuity of the flux function. This is possible since u_F is a *given* constant (or possibly a given (control) function of t). Thus, the governing conservation law can be written as

$$u_t + g(u,x)_x = 0, \quad g(u,x) := \begin{cases} q_L(u - u_F) + b(u) & \text{for } x < 0, \\ q_R(u - u_F) + b(u) & \text{for } x \geq 0. \end{cases} \tag{1.8}$$

Note that the *injection* of material of given concentration and at given rate leads to a homogeneous conservation law with discontinuous flux. This property has made the clarifier-thickener problem tractable.

In the present work, we extend the clarifier-thickener model to the case that we also extract material at a fixed location. To elucidate the problem, consider a

column with an upwards directed bulk flow of $Q_{\mathrm{R}} < 0$. At depth $x = 0$, we divide the flow into a discharge flow $Q_{\mathrm{D}} < 0$ and the remaining upwards directed bulk flow Q_{L} with $Q_{\mathrm{R}} < Q_{\mathrm{L}} < 0$, see the right diagram of Figure 1. Considering that the concentration $u(0,t)$ of the suspension extracted is unknown beforehand and defining $q_{\mathrm{R}} := Q_{\mathrm{R}}/\mathcal{S}$ and $q_{\mathrm{L}} := Q_{\mathrm{L}}/\mathcal{S}$, we obtain instead of (1.8) the equation

$$u_t + h(u,x)_x = \delta(x)(q_{\mathrm{R}} - q_{\mathrm{L}})u(x,t), \quad h(u,x) = \begin{cases} q_{\mathrm{L}}u + b(u) & \text{for } x < 0, \\ q_{\mathrm{R}}u + b(u) & \text{for } x > 0. \end{cases} \tag{1.9}$$

Note that we cannot use the Heaviside function in the same way as in (1.7), since now the solution value $u(x,t)$ replaces the constant u_{F} in the singular term. This difference justifies studying the sink term problem in its own right, rather than claiming that it is just analogous to the source term problem. This view is further supported by the observation that the so-called crossing condition [34], which ensures uniqueness of an entropy solution of the initial value problem, is satisfied for (1.8) but may be violated for (1.9), so uniqueness is not an obvious issue here in view of our previous results.

To further motivate this research, let us mention that several researchers in chemical engineering and mineral processing have reported experiments with separation devices that can be modeled by the extended clarifier-thickener concept. For example, Galvin and co-workers [26, 27, 28, 45] have developed a so-called reflux classifier, a device that allows to separate the solids of a polydisperse suspension into different size classes by pumping it from below into a vessel with internal inclined plates, and by tapping the device at different heights to obtain different size distributions. Roughly speaking, a mathematical model for the operation of this equipment is equivalent to a one-dimensional unit that has a feed source at its bottom, and several discharge sink terms located in different heights above. It is clear that if we know how to properly handle one sink term, then we can also deal with any array of them. On the other hand, Nasr-El-Din and co-workers [42, 43, 44] and Spannenberg et al. [50] study vertical columns for the gravity separation of polydisperse suspensions that have a feed source at a central depth level, and which are tapped near the top and bottom ends. This shows that the study of sink terms is highly relevant for engineering applications.

To put our paper in the proper mathematical perspective, let us first mention that equation (1.9), which includes a new sink term, after slight notational simplification, forms the so-called *reduced problem* studied in our paper. This is opposed to the *full extended clarifier-thickener model* which besides the sink term also includes singular source terms and flux discontinuities; however, from [10] we already know how to deal with the latter ingredients. Assuming for simplicity that $q_{\mathrm{R}} - q_{\mathrm{L}} = 1$ and writing q for q_{L}, we may formally rewrite the governing equation (1.9) of the reduced problem as a non-strictly hyperbolic system

$$\begin{aligned} &a_t = 0, \quad u_t + F(a,u)_x - G(a,u)a_x = 0, \quad x \in \mathbb{R}, \quad t \geq 0; \\ &(a,u)(0,x) = (a_0(x), u_0(x)), \quad x \in \mathbb{R}, \end{aligned} \tag{1.10}$$

where we define $a_0(x) := H(x)$, $G(a,u) := u$ and $F(a,u) := (q+a)u + b(u)$.

In passing, let us mention that if we set $F(a,u) := f(a,u)$, $G \equiv 0$ and $a_0(x) := \gamma(x)$, then (1.10) is equivalent to the Cauchy problem for (1.1) in the case of a scalar discontinuous parameter $\gamma(x)$. The resulting triangular hyperbolic system has been

the starting point of several analyses of conservation laws with discontinuous flux, see e.g. [7, 20, 24, 29, 30, 36, 37].

Systems of the type (1.10) with $G \not\equiv 0$ were analyzed in a recent paper by Amadori et al. [2]. These authors solve the Riemann problem for (1.10) and prove that a Godunov scheme, which relies on the Riemann solver as building block, converges. They address uniqueness by means of a Kružkov-type technique. However, our reduced model is not a sub-case included in the analysis of [2], since some of the structural assumptions stated in [2] are not satisfied in our case. For example, their requirement (P_4), stating that $F_a - G \neq 0$ for all (a, u) with $F_u(a, u) = 0$, is obviously not satisfied, since $F_a - G \equiv 0$ in our case. Let us point out that their uniqueness result does not hold for a discontinuous coefficient a, while our approach does include uniqueness.

The remainder of this paper is organized as follows. The extended clarifier-thickener model, which includes combinations of source and sink terms as well as transitions to linear transport fluxes outside the proper tank (such transitions have been omitted in this section for sake of simplicity of the argument), is derived in Section 2. The result is a conservation law with a flux that is discontinuous at the source and transition points, but *not* at the location of the sink term, and which has a non-conservative linear flux term. Furthermore, we derive the above-mentioned reduced problem that includes the singularities caused by the new sink term only. It is sufficient to study the reduced problem since the other singularities can be dealt with by known methods [10].

The reduced problem is analyzed further on in Section 3. We first introduce a definition of entropy solutions for the reduced problem. This definition consists of two separate integral inequalities (involving standard Kružkov-type [38] entropy functions and fluxes), which refer to the two half-spaces on either side of the singular sink term sitting at $x = 0$. The solutions on both sides are coupled by a series of jump conditions valid across $x = 0$. We then prove by an adaptation of the "doubling of variables" argument [38] that these jump conditions imply an L^1 stability property, which immediately implies uniqueness of an entropy solution. In Section 4, we introduce an explicit finite difference scheme for the complete model. The scheme is the upwind scheme introduced in [10] extended by an upwind discretization of the non-conservative product arising from the sink term. We prove that the solution produced by the scheme remains in the interval $[0, 1]$, that the scheme is monotone under a suitable CFL condition, and that it satisfies a time continuity property. In Section 5 we focus on the reduced problem and demonstrate that the scheme satisfies a spatial variation bound. This spatial variation property is established by a technique which relies entirely on the time continuity estimate and is robust enough to yield compactness also in the discontinuous flux case. Finally, starting from a discrete entropy inequality, using the monotonicity property and proceeding as in the proof of the Lax-Wendroff theorem, we show that the scheme converges to an entropy solution. The analysis is summarized in a theorem that states the well-posedness of the reduced problem. Combining the new result with the treatment in [10], this implies that the full extended clarifier-thickener model, and not just the reduced problem, is well-posed.

At a fixed spatial position, the flux appearing in both the reduced problem and the full clarifier-thickener model is a sum of a nonlinear term and several linear terms. There are several different ways to define suitable schemes for the

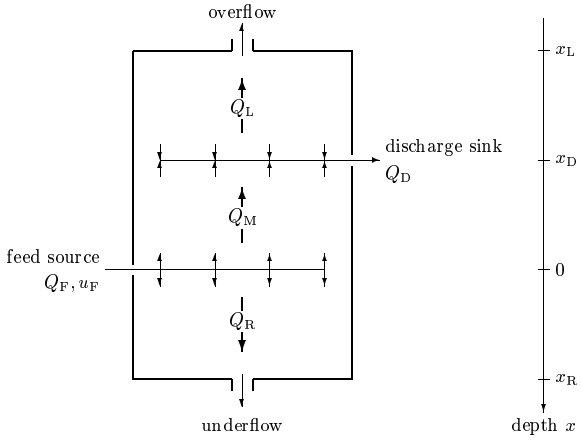

FIGURE 2. The extended clarifier-thickener setup showing the known bulk flows and control variables.

resulting equation by combining upwind discretizations for the linear terms with an Engquist-Osher type numerical flux for the remaining nonlinear portion. Based on this observation, we introduce in Section 6, two different variants of the scheme. The new variants are referred to as "Scheme 1" and "Scheme 3", respectively, while the scheme analyzed so far is referred to as "Scheme 2". (This nomenclature anticipates the observed ranking in performance.) The analysis of Scheme 2 in Sections 4 and 5 also fully holds for Scheme 1. The convergence result also applies to Scheme 3, while the entropy analysis may require different arguments. The three schemes are compared in Section 7 for several cases of both the reduced problem and the complete model. It turns out that although all three schemes converge to the entropy solution, they significantly differ in the degree of numerical diffusion introduced. Scheme 1 is very easy to implement, but turns out to be very diffusive, especially for steady-state jumps generated by the discontinuous coefficients of the flux, while Scheme 3 produces sharp resolution.

2. The extended clarifier-thickener model

2.1. **Bulk flow variables.** Consider the extended clarifier-thickener drawn in Figure 2, which is supposed to have a constant cross-sectional area $\mathcal{S}$. This setup is similar to that considered in [7, 9, 10], but is equipped with an additional sink located at depth x_{D}. This (of course, idealized) unit is operated as follows.

At depth $x = 0$, suspension is fed into the unit at a volume rate $Q_{\mathrm{F}}(t) \geq 0$. The feed suspension is loaded with solids of the volume fraction $u_{\mathrm{F}}(t)$, where $u_{\mathrm{F}}(t) \in [0, u_{\max}]$, and $u_{\max}$ is a maximum solids concentration. At $x = 0$, the feed flow divides into an upwards-directed and a downwards-directed bulk flow. We assume that the underflow volume rate $Q_{\mathrm{R}}(t) \geq 0$ is also prescribed, and that $Q_{\mathrm{R}}(t) \leq Q_{\mathrm{F}}(t)$. Thus, the signed volume rate of the upwards-directed bulk flow immediately above the feed source is

$$Q_{\mathrm{M}}(t) = Q_{\mathrm{R}}(t) - Q_{\mathrm{F}}(t) \leq 0. \tag{2.1}$$

At depth $x = x_{\mathrm{D}}$, $x_{\mathrm{L}} < x_{\mathrm{D}} < 0$, a discharge sink is located. Suspension is extracted from the column at a signed volume rate $Q_{\mathrm{D}}(t) \leq 0$, where we assume

$Q_{\mathrm{D}}(t) \geq Q_{\mathrm{M}}(t)$. Above the discharge sink, for $x_{\mathrm{L}} \leq x \leq x_{\mathrm{D}}$, there is an upwards directed bulk flow with the volume rate

$$Q_{\mathrm{L}}(t) = Q_{\mathrm{M}}(t) - Q_{\mathrm{D}}(t) = Q_{\mathrm{R}}(t) - Q_{\mathrm{F}}(t) - Q_{\mathrm{D}}(t) \leq 0. \tag{2.2}$$

Summarizing, we prescribe the volume rates $Q_{\mathrm{F}}(t)$, $Q_{\mathrm{R}}(t)$ and $Q_{\mathrm{D}}(t)$ and the feed concentration $u_{\mathrm{F}}(t)$ as independent control variables. From these we calculate the dependent control variables $Q_{\mathrm{M}}(t)$ and $Q_{\mathrm{L}}(t)$ by (2.1) and (2.2), respectively.

For the remainder of the paper, we simply assume that all control variables are constant with respect to t, and we introduce the velocities $q_c := Q_c/\mathcal{S}$, $c \in \{\mathrm{D}, \mathrm{F}, \mathrm{L}, \mathrm{M}, \mathrm{R}\}$. Disregarding for a moment the presence of solids sources and sinks but appropriately taking into account these bulk flow velocities and exclusively utilizing independent control variables, we can write the flux function as

$$\tilde{g}(u,x) = \begin{cases} (q_{\mathrm{R}} - q_{\mathrm{F}} - q_{\mathrm{D}})u & \text{for } x \leq x_{\mathrm{L}}, \\ (q_{\mathrm{R}} - q_{\mathrm{F}} - q_{\mathrm{D}})u + b(u) & \text{for } x_{\mathrm{L}} < x \leq x_{\mathrm{D}}, \\ (q_{\mathrm{R}} - q_{\mathrm{F}})u + b(u) & \text{for } x_{\mathrm{D}} < x \leq 0, \\ q_{\mathrm{R}}u + b(u) & \text{for } 0 < x \leq x_{\mathrm{R}}, \\ q_{\mathrm{R}}u & \text{for } x > x_{\mathrm{R}}. \end{cases} \tag{2.3}$$

2.2. **Solids feed and sink terms.** Including now the solids feed and sink mechanisms, we obtain the conservation law with source terms

$$\begin{aligned} u_t + \tilde{g}(u,x)_x =& q_{\mathrm{F}}u_{\mathrm{F}}\delta(x) + q_{\mathrm{D}}u(x,t)\delta(x - x_{\mathrm{D}}) \\ =& q_{\mathrm{F}}u_{\mathrm{F}}H'(x) + q_{\mathrm{D}}\big(H(x - x_{\mathrm{D}})u(x,t)\big)_x - q_{\mathrm{D}}H(x - x_{\mathrm{D}})u_x(x,t), \end{aligned} \tag{2.4}$$

where $\delta(\cdot)$ denotes the Dirac delta mass. Next, absorbing the term $q_{\mathrm{F}}u_{\mathrm{F}}H'(x) + q_{\mathrm{D}}(H(x - x_{\mathrm{D}})u(x,t))_x$ into the convective flux yields the equation

$$u_t + g(u,x)_x = -q_{\mathrm{D}}H(x - x_{\mathrm{D}})u_x(x,t),$$

where, after defining $\tilde{q}_{\mathrm{R}} := q_{\mathrm{R}} - q_{\mathrm{D}}$ and adding the constant $-q_{\mathrm{L}}u_{\mathrm{F}}$, we obtain the flux function

$$g(u,x) = \begin{cases} (\tilde{q}_{\mathrm{R}} - q_{\mathrm{F}})(u - u_{\mathrm{F}}) & \text{for } x \leq x_{\mathrm{L}}, \\ (\tilde{q}_{\mathrm{R}} - q_{\mathrm{F}})(u - u_{\mathrm{F}}) + b(u) & \text{for } x_{\mathrm{L}} < x \leq 0, \\ \tilde{q}_{\mathrm{R}}(u - u_{\mathrm{F}}) + b(u) & \text{for } 0 < x \leq x_{\mathrm{R}}, \\ \tilde{q}_{\mathrm{R}}(u - u_{\mathrm{F}}) & \text{for } x > x_{\mathrm{R}}, \end{cases} \tag{2.5}$$

i.e. the flux is continuous across $x = x_{\mathrm{D}}$. Defining the discontinuous parameters

$$\gamma^1(x) := \begin{cases} 0 & \text{for } x \notin [x_{\mathrm{L}}, x_{\mathrm{R}}], \\ 1 & \text{for } x \in [x_{\mathrm{L}}, x_{\mathrm{R}}], \end{cases} \quad \gamma^2(x) := \begin{cases} \tilde{q}_{\mathrm{R}} - q_{\mathrm{F}} & \text{for } x < 0, \\ \tilde{q}_{\mathrm{R}} & \text{for } x > 0, \end{cases} \tag{2.6}$$

$$\gamma^3(x) := \begin{cases} 0 & \text{for } x < x_{\mathrm{D}}, \\ -q_{\mathrm{D}} > 0 & \text{for } x > x_{\mathrm{D}} \end{cases} \tag{2.7}$$

and using $\boldsymbol{\gamma}(x) := (\gamma^1(x), \gamma^2(x))$, we can rewrite (2.5) as

$$f\big(\boldsymbol{\gamma}(x), u\big) := g(u,x) = \gamma^1(x)b(u) + \gamma^2(x)(u - u_{\mathrm{F}}), \tag{2.8}$$

so that the final governing balance law takes the form

$$u_t + f\big(\boldsymbol{\gamma}(x), u\big)_x = \gamma^3(x)u_x. \tag{2.9}$$

Here the flux $f(\boldsymbol{\gamma}(x), u)$ incorporates the batch flux, along with the source term and the discontinuities at the discharge and overflow levels. In other words, if we set the right side of (2.9) to zero, we have essentially the PDE analyzed in [10].

2.3. **Reduced problem.** The flux discontinuities at $x = x_{\mathrm{L}}$, $x = 0$ and $x = x_{\mathrm{R}}$ are the same as in [10]. In view of previous works, they can be incorporated easily once the discontinuity near $x = x_{\mathrm{D}}$, where the sink is located, can be handled. The analysis in this paper is therefore focused on the following problem, where the sink has been moved to $x = 0$:

$$u_t + \varphi(u)_x - \gamma(x)u_x = 0, \quad x \in \mathbb{R},\ t > 0, \tag{2.10}$$

$$u(x,0) = u_0(x), \quad x \in \mathbb{R},\ u_0 \in [0, u_{\max}], \tag{2.11}$$

$$\varphi(u) = qu + b(u), \quad \gamma(x) = \begin{cases} 0 =: \gamma_- & \text{for } x < 0, \\ \gamma_+ & \text{for } x > 0, \end{cases} \tag{2.12}$$

where we assume that the velocities have been normalized such that q_{D} (in the original problem description) equals $-\gamma_+$, and that $q \leq -0$. The last restriction is required in the stability and uniqueness analysis.

The function $b(u)$ is assumed to be Lipschitz continuous, positive for $u \in (0,1)$, and to vanish for $u \notin (0,1)$. We assume that $b(u)$ is twice differentiable in $(0,1)$, that $b'(u)$ vanishes at exactly one location $u = u_b^* \in (0,1)$, where the function has a maximum, and that $b''(u)$ vanishes at no more than one inflection point in $u_{\mathrm{infl}} \in (0,1)$; if such a point is present, we assume that $u_{\mathrm{infl}} \in (u_{\max}, 1)$. These assumptions are valid for the flux density function (1.4) with $u_{\max} = 1$. With these assumptions on $b(u)$ and the sign of q, the flux $\varphi(u) = b(u) + qu$ will have a single maximum located at the point $u^* \in [0,1]$, and φ will be non-decreasing on $[0, u^*]$ and non-increasing on $[u^*, 1]$. Note that we refer to (2.10)–(2.12) as *reduced problem*, while (2.6)–(2.9) and (2.11) form the *full extended clarifier-thickener model*.

3. Entropy solution and uniqueness analysis of the reduced problem

Before stating the definition of entropy solution, we recall the notation $a \vee b := \max\{a, b\}$, $a \wedge b := \min\{a, b\}$.

Definition 3.1 (Entropy solution)**.** *A function $u : \Pi_T \mapsto \mathbb{R}$ is an entropy solution of the initial value problem* (2.10)–(2.12) *if it satisfies the following conditions:*

(**D**.1) *$u \in L^1(\Pi_T) \cap BV(\Pi_T)$ and $u(x,t) \in [0,1]$ for a.e. $(x,t) \in \Pi_T$.*

(**D**.2) *If $0 \leq \psi \in \mathcal{D}(\Pi_T)$ vanishes for $x > 0$, then*

$$\iint_{\Pi_T} \Big(|u - c|\, \psi_t + \operatorname{sgn}(u - c)\big(\varphi(u) - \varphi(c)\big)\psi_x \Big)\, dt\, dx \geq 0 \quad \forall c \in \mathbb{R}, \tag{3.1}$$

and if $0 \leq \psi \in \mathcal{D}(\Pi_T)$ vanishes for $x < 0$, then

$$\iint_{\Pi_T} \Big(|u - c|\, \psi_t + \operatorname{sgn}(u - c)\big(\varphi(u) - \varphi(c) - \gamma_+(u - c)\big)\psi_x \Big)\, dt\, dx \geq 0 \quad \forall c \in \mathbb{R}. \tag{3.2}$$

(**D**.3) *With the abbreviation $u_\pm = u(0\pm, t)$, the following jump conditions hold at $x = 0$ for a.e. $t \in (0,T)$:*

If $u_- \leq c \leq u_+$, then

$$\varphi(u_+) - \varphi(c) \leq \gamma_+(u_+ - c), \tag{3.3}$$

$$\varphi(u_-) - \varphi(c) \leq 0, \tag{3.4}$$

and if $u_- \geq c \geq u_+$, *then*

$$\varphi(u_+) - \varphi(c) \geq \gamma_+(u_+ - c), \tag{3.5}$$

$$\varphi(u_-) - \varphi(c) \geq 0. \tag{3.6}$$

(**D**.4) *The initial condition is satisfied in the following strong* L^1 *sense:*

$$\operatorname*{ess\,lim}_{t\downarrow 0} \int_{\mathbb{R}} \big|u(x,t) - u_0(x)\big| dx = 0. \tag{3.7}$$

Remark 3.1. For the full extended clarifier-thickener model captured by equation (2.9), we would have to replace the condition $u \in BV(\Pi_T)$ by the weaker condition $u \in BV_t(\Pi_T)$. Here $BV_t(\Pi_T)$ is the class of functions $W(x,t)$ with $\partial_t W$ being a finite measure. The presence of the discontinuities in the parameter vector $\boldsymbol{\gamma}$ makes it difficult (in the case of the extended model (2.9)) to get global control of the spatial variation of the solution u.

Remark 3.2. It is clear from (3.1), (3.2) that if u is an entropy solution in the sense of Definition 3.1, then for $x < 0$, u is an entropy solution in the usual Kružkov sense of the conservation law $u_t + \varphi(u)_x = 0$, while for $x > 0$, u is an entropy solution (in the usual Kružkov sense) of the conservation law $u_t + (\varphi(u) - \gamma_+ u)_x = 0$.

Remark 3.3. In equation (2.10) for the reduced problem, we have a so-called non-conservative product. More specifically, we have what amounts to a δ function, u_x, multiplied by a discontinuous function $\gamma(x)$. We expect a jump condition of the form

$$\varphi(u_+) - \varphi(u_-) = \bar{\gamma}(u_+ - u_-), \tag{3.8}$$

where $\bar{\gamma}$ is some intermediate value of γ, i.e. $0 = \gamma_- \leq \bar{\gamma} \leq \gamma_+$. In fact, when $u_- \leq u_+$, we can take $c = u_-$ in (3.3) and then $c = u_+$ in (3.4) to get

$$0 \leq \varphi(u_+) - \varphi(u_-) \leq \gamma_+(u_+ - u_-),$$

which implies (3.8). Similarly, when $u_- \geq u_+$, we can take $c = u_-$ in (3.5) and then $c = u_+$ in (3.6) to get

$$\gamma_+(u_+ - u_-) \leq \varphi(u_+) - \varphi(u_-) \leq 0,$$

which again implies (3.8).

From the jump conditions in Definition 3.1 we derive the following additional jump conditions.

Lemma 3.1. *Let* u *be an entropy solution in the sense of Definition 3.1. The following jump conditions hold at* $x = 0$ *for a.e.* $t \in (0,T)$ *for which* $u_-(t) \neq u_+(t)$*:*

$$0 \leq \frac{\varphi(u_+) - \varphi(u_-)}{u_+ - u_-} \leq \gamma_+, \tag{3.9}$$

$$u_+ < u_- \Rightarrow u_+ < u_- \leq u^*, \tag{3.10}$$

where u^* *is defined towards the end of Subsection 2.3.*

Proof. To prove (3.9), first take the case where $u_- < u_+$. Letting $c = u_-$ in (3.3), and then $c = u_+$ in (3.4), yields the inequalities

$$\varphi(u_+) - \varphi(u_-) \leq \gamma_+(u_+ - u_-), \quad \varphi(u_+) - \varphi(u_-) \geq 0.$$

Inequality (3.9) follows immediately from these two inequalities. If $u_+ < u_-$, we arrive at (3.9) by a similar calculation, this time taking $c = u_-$ in (3.5), and then $c = u_+$ in (3.6).

To prove (3.10), it suffices to show that neither of the orderings $u_+ \le u^* < u_-$, $u^* < u_+ < u_-$ is possible. If $u_+ \le u^* < u_-$, letting $c = u^*$ in (3.6) results in $\varphi(u^*) - \varphi(u_-) \le 0$, which contradicts our assumptions about the shape of the graph of $u \mapsto \varphi(u)$. If $u^* < u_+ < u_-$, letting $c = u^+$ in (3.6) yields $\varphi(u_+) - \varphi(u_-) \le 0$. Since φ is strictly decreasing on $[u^*, 1]$, this is a contradiction. □

Remark 3.4. In the absence of the sink term ($\gamma_+ = 0$), the jump condition (3.9) becomes

$$\frac{\varphi(u_+) - \varphi(u_-)}{u_+ - u_-} = 0,$$

which is the usual Rankine-Hugoniot condition satisfied by a zero-speed discontinuity for the conservation law $u_t + \varphi(u)_x = 0$. Based on this observation, it seems that (3.9) is playing the role of a Rankine-Hugoniot condition for a steady jump located at $x = 0$ where the delta-function due to the sink term is concentrated.

We are now ready to prove that entropy solutions are L^1 stable and hence unique.

Theorem 3.1 (L^1 stability and uniqueness)**.** *Let u and v be two entropy solutions in the sense of Definition 3.1 of the initial value problem* (2.10)–(2.12) *with initial data u_0 and v_0, respectively. Then, for a.e. $t \in (0, T)$,*

$$\int_{\mathbb{R}} \big|u(x,t) - v(x,t)\big|\, dx \le \int_{\mathbb{R}} \big|u_0(x) - v_0(x)\big|\, dx.$$

In particular, there exists at most one entropy solution of the reduced model (2.10)–(2.12)*.*

Proof. Using standard methods and in particular the doubling of variables technique [38], one can derive from (3.1) and (3.2) the following pair of integral inequalities for u and v:

$$\begin{aligned} &\forall \psi^1 \in \mathcal{D}(\Pi_T), \quad \psi^1(x,t) = 0 \text{ for } x > 0\text{:} \\ &\iint_{\Pi_T} \Big(|u - v| \psi^1_t + \operatorname{sgn}(u - v)\big(\varphi(u) - \varphi(v)\big)\psi^1_x \Big)\, dt\, dx \ge 0, \end{aligned} \tag{3.11}$$

$$\begin{aligned} &\forall \psi^2 \in \mathcal{D}(\Pi_T), \quad \psi^2(x,t) = 0 \text{ for } x < 0\text{:} \\ &\iint_{\Pi_T} \Big(|u - v| \psi^2_t + \operatorname{sgn}(u - v)\big(\varphi(u) - \varphi(v) - \gamma_+(u - v)\big)\psi^2_x \Big)\, dt\, dx \ge 0. \end{aligned} \tag{3.12}$$

Now let us choose $\psi^1(x,t) = \Phi(t)\nu_h(x)$ and $\psi^2(x,t) = \Phi(t)\mu_h(x)$, where $\Phi \in C_0^2(0,T)$, $\Phi(\cdot) \ge 0$, and $\{\mu_h\}_{h>0}$ and $\{\nu_h\}_{h>0}$ are standard boundary layer sequences that are assumed to satisfy $\mu_h \in C^1(\mathbb{R})$, $\mu_h(x) = 0$ for $x \le 0$, $0 \le \mu_h(\cdot) \le 1$, $\mu_h(x) = 1$ for $x > h$, $|\mu_h'(\cdot)| \le C/h$, where C is a constant independent of h, and $\nu_h(x) := 1 - \mu_h(x + h)$. Since the solutions u and v possess traces with respect to $x \to 0$, we obtain by inserting ψ^1 and ψ^2 in (3.11) and (3.12), letting $h \to 0$, and considering that for all h, ψ^1 vanishes for $x \ge 0$, while ψ^2 vanishes for $x \le 0$, the

inequalities

$$\begin{aligned}\int_{-\infty}^{0}\int_0^T |u-v|\Phi'(t)\,dt\,dx \\ \geq \int_0^T \operatorname{sgn}(v_- - u_-)\big(\varphi(v_-)-\varphi(u_-)\big)\Phi(t)\,dt,\end{aligned} \tag{3.13}$$

$$\begin{aligned}\int_0^{\infty}\int_0^T |u-v|\Phi'(t)\,dt\,dx \\ \geq -\int_0^T \operatorname{sgn}(v_+ - u_+)\big(\varphi(v_+)-\varphi(u_+)-\gamma_+(v_+-u_+)\big)\Phi(t)\,dt.\end{aligned} \tag{3.14}$$

In a standard fashion, let now ω_h be a non-negative C^∞ mollifier with support on $(-h,h)$ and $\|\omega_h\|_{L^1(\mathbb{R})}=1$. Then let $\varrho_h(x):=\int_0^x \omega_h(\xi)\,d\xi$ and take $\Phi(t):=\varrho_h(t-t_1)-\varrho_h(t-t_2)$, where $0\leq t_1<t_2\leq T$. Taking $h\to 0$, we obtain

$$\begin{aligned}&\int_{\mathbb{R}}\big|u(\cdot,t_2)-v(\cdot,t_2)\big|\,dx-\int_{\mathbb{R}}\big|u(\cdot,t_1)-v(\cdot,t_1)\big|\,dx\leq E,\\ &E:=\int_{t_1}^{t_2}\Big\{\operatorname{sgn}(v_+-u_+)\big(\varphi(v_+)-\varphi(u_+)-\gamma_+(v_+-u_+)\big)\\ &\qquad\qquad-\operatorname{sgn}(v_--u_-)\big(\varphi(v_-)-\varphi(u_-)\big)\Big\}dt.\end{aligned} \tag{3.15}$$

To prove the L^1 contraction property, we must verify that $E\leq 0$ by showing that the jump conditions ensure that the integrand in (3.15) is non-positive for almost all $t\in(0,T)$. To this end, we give a name to the integrand in E at $x=0$ for almost every $t\in(0,T)$:

$$\begin{aligned}S:=&\operatorname{sgn}(v_+-u_+)\left(\varphi(v_+)-\gamma_+v_+-\varphi(u_+)+\gamma_+u_+\right)\\ &-\operatorname{sgn}(v_--u_-)\left(\varphi(v_-)-\varphi(u_-)\right).\end{aligned} \tag{3.16}$$

Our goal now is to show that $S\leq 0$. We prove this by examining the cases corresponding to the ordering among the four numbers u_-,u_+,v_-,v_+. There are 24 such cases, but we can eliminate half of them, since interchanging u_- with v_- and u_+ with v_+ leads to the same proofs, only with different labels.

Case 1. $u_-\leq v_-\leq u_+\leq v_+$. In this case

$$S=\varphi(v_+)-\gamma_+v_+-\varphi(u_+)+\gamma_+u_+-\big(\varphi(v_-)-\varphi(u_-)\big).$$

Taking $c=v_-$ in (3.4), we get

$$\varphi(u_-)-\varphi(v_-)\leq 0.$$

Interchanging u and v and setting $c=u_+$ in (3.5), we obtain $\varphi(v_+)-\varphi(u_+)-\gamma_+(v_+-u_+)\leq 0$, which makes it clear that $S\leq 0$.

Case 2. $u_-\leq v_-\leq v_+\leq u_+$. In this case

$$\begin{aligned}S&=\varphi(u_+)-\gamma_+u_+-\varphi(v_+)+\gamma_+v_+-\big(\varphi(v_-)-\varphi(u_-)\big)\\ &\leq\varphi(u_+)-\gamma_+u_+-\varphi(v_+)+\gamma_+v_+.\end{aligned}$$

Here we have used the fact that $\varphi(v_-)-\varphi(u_-)\geq 0$, which results by taking $c=v_-$ in (3.4). Now letting $c=v_+$ in (3.3), we get $\varphi(u_+)-\varphi(v_+)\leq\gamma_+(u_+-v_+)$, making it clear that $S\leq 0$.

Case 3. $u_-\leq u_+\leq v_-\leq v_+$. In this case

$$S=\varphi(v_+)-\gamma_+v_+-\varphi(u_+)+\gamma_+u_+-\big(\varphi(v_-)-\varphi(u_-)\big).$$

From (3.9), $\varphi(u_-) - \varphi(u_+) \le 0$, and so

$$S \le \varphi(v_+) - \varphi(v_-) - \gamma_+(v_+ - u_+) \le \varphi(v_+) - \varphi(v_-) - \gamma_+(v_+ - v_-).$$

Taking $c = v_-$ in (3.3), it is now clear that $S \le 0$.

Case 4. $u_- \le u_+ \le v_+ \le v_-$. In this case

$$S = \varphi(v_+) - \gamma_+ v_+ - \varphi(u_+) + \gamma_+ u_+ - \big(\varphi(v_-) - \varphi(u_-)\big).$$

From (3.9), $\varphi(u_-) - \varphi(u_+) \le 0$, $\varphi(v_+) - \varphi(v_-) \le 0$ and so

$$S \le -\gamma_+(v_+ - u_+) \le 0.$$

Case 5. $u_- \le v_+ \le v_- \le u_+$. In this case

$$S = \varphi(u_+) - \gamma_+ u_+ - \varphi(v_+) + \gamma_+ v_+ - \big(\varphi(v_-) - \varphi(u_-)\big).$$

Taking $c = v_+$ in (3.3), and then $c = v_-$ in (3.4), we find that

$$\varphi(u_+) - \varphi(v_+) - \gamma_+(u_+ - v_+) \le 0, \quad \varphi(v_-) - \varphi(u_-) \ge 0,$$

which clearly yields $S \le 0$.

Case 6. $u_- \le v_+ \le u_+ \le v_-$. In this case

$$S = \varphi(u_+) - \gamma_+ u_+ - \varphi(v_+) + \gamma_+ v_+ - \big(\varphi(v_-) - \varphi(u_-)\big).$$

Letting $c = v_+$ in (3.3) results in

$$\varphi(u_+) - \varphi(v_+) \le \gamma_+(u_+ - v_+),$$

and so

$$S \le -\big(\varphi(v_-) - \varphi(u_-)\big).$$

Taking $c = v_+$ in (3.4) gives $\varphi(v_+) - \varphi(u_-) \ge 0$. Also, from (3.9), we see that $\varphi(v_-) \ge \varphi(v_+)$. Combining these inequalities gives $\varphi(v_-) - \varphi(u_-) \ge 0$, and thus $S \le 0$.

Case 7. $u_+ \le u_- \le v_- \le v_+$. In this case

$$\begin{aligned} S &= \varphi(v_+) - \gamma_+ v_+ - \varphi(u_+) + \gamma_+ u_+ - \big(\varphi(v_-) - \varphi(u_-)\big) \\ &\le \varphi(v_+) - \gamma_+ v_+ - \varphi(u_+) + \gamma_+ u_+ - \big(\varphi(v_-) - \varphi(u_-)\big) + \gamma_+ v_- - \gamma_+ u_- \\ &= \varphi(v_+) - \varphi(v_-) - \gamma_+(v_+ - v_-) - \big(\varphi(u_+) - \varphi(u_-) - \gamma_+(u_+ - u_-)\big). \end{aligned} \tag{3.17}$$

By (3.9), we have the inequalities

$$\varphi(v_+) - \varphi(v_-) - \gamma_+(v_+ - v_-) \le 0, \quad \varphi(u_+) - \varphi(u_-) - \gamma_+(u_+ - u_-) \ge 0,$$

yielding $S \le 0$.

Case 8. $u_+ \le u_- \le v_+ \le v_-$. In this case

$$S = \varphi(v_+) - \gamma_+ v_+ - \varphi(u_+) + \gamma_+ u_+ - \big(\varphi(v_-) - \varphi(u_-)\big). \tag{3.18}$$

By (3.9), $\varphi(v_+) \le \varphi(v_-)$, which results in the inequality

$$S \le \varphi(u_-) - \varphi(u_+) - \gamma_+(v_+ - u_+) \le \varphi(u_-) - \varphi(u_+) - \gamma_+(u_- - u_+).$$

Taking $c = u_-$ in (3.5), we find that $\varphi(u_-) - \varphi(u_+) - \gamma_+(u_- - u_+) \le 0$, yielding $S \le 0$.

Case 9. $v_+ \le u_- \le v_- \le u_+$. In this case

$$S = \varphi(u_+) - \gamma_+ u_+ - \varphi(v_+) + \gamma_+ v_+ - \big(\varphi(v_-) - \varphi(u_-)\big). \tag{3.19}$$

Taking $c = u_-$ in (3.5) gives $\varphi(v_+) - \varphi(u_-) \ge \gamma_+(v_+ - u_-)$, which we can rearrange as $-\varphi(v_+) + \varphi(u_-) + \gamma_+ v_+ \le \gamma_+ u_-$. From this it follows that

$$S \le \varphi(u_+) - \varphi(v_-) - \gamma_+ u_+ + \gamma_+ u_-.$$

Now (3.10) tells us that $v_+ \le v_- \le u^*$. Recalling that $u \mapsto \varphi(u)$ is non-decreasing on $[0, u^*]$, and that $v_+ \le u_- \le v_-$, we find that $\varphi(u_-) \le \varphi(v_-)$, and so

$$S \le \varphi(u_+) - \varphi(u_-) - \gamma_+ u_+ + \gamma_+ u_-.$$

The right side of this last inequality is non-positive due to (3.9), and so $S \le 0$.

Case 10. $v_+ \le u_- \le u_+ \le v_-$. In this case

$$S = \varphi(u_+) - \gamma_+ u_+ - \varphi(v_+) + \gamma_+ v_+ - \big(\varphi(v_-) - \varphi(u_-)\big). \tag{3.20}$$

Taking $c = u_+$ in (3.5) gives $\varphi(v_+) - \varphi(u_+) \ge \gamma_+(v_+ - u_+)$, from which we derive $S \le \varphi(u_-) - \varphi(v_-)$. From (3.10) we have that $v_+ \le v_- \le u^*$. Since also $u_- \le v_- \le u^*$, we see that $\varphi(u_-) \le \varphi(v_-)$, yielding $S \le 0$.

Case 11. $u_+ \le v_- \le u_- \le v_+$. In this case

$$S = \varphi(v_+) - \gamma_+ v_+ - \varphi(u_+) + \gamma_+ u_+ - \big(\varphi(u_-) - \varphi(v_-)\big). \tag{3.21}$$

Taking $c = u_-$ in (3.3) results in

$$\varphi(v_+) - \varphi(u_-) - \gamma_+ v_+ \le -\gamma_+ u_-,$$

which in turn gives us

$$S \le -\varphi(u_+) + \gamma_+ u_+ + \varphi(v_-) - \gamma_+ u_-.$$

From (3.10) we have that $u_+ \le u_- \le u^*$. Since also $v_- \le u_- \le u^*$, we have $\varphi(v_-) \le \varphi(u_-)$, and so

$$S \le -\varphi(u_+) + \gamma_+ u_+ + \varphi(u_-) - \gamma_+ u_- = \varphi(u_-) - \varphi(u_+) - \gamma_+(u_- - u_+).$$

This last quantity is non-positive, due to (3.9), resulting in $S \le 0$.

Case 12. $u_+ \le v_+ \le u_- \le v_-$. In this case

$$S = \varphi(v_+) - \gamma_+ v_+ - \varphi(u_+) + \gamma_+ u_+ - \big(\varphi(v_-) - \varphi(u_-)\big). \tag{3.22}$$

Taking $c = v_+$ in (3.5) results in

$$\varphi(v_+) - \varphi(u_+) - \gamma_+(v_+ - u_+) \le 0,$$

which in turn gives us $S \le \varphi(u_-) - \varphi(v_-)$. From (3.10) we have that $v_+ \le v_- \le u^*$. Since also $u_- \le v_- \le u^*$, we have $\varphi(u_-) \le \varphi(v_-)$, making it clear that $S \le 0$. □

4. Numerical scheme and some properties

In this section we describe our finite difference scheme as it applies to the full model (2.6)–(2.9), and prove two of its properties. In the section that follows we use the scheme to prove the existence of an entropy solution for the reduced model.

We begin the definition of the difference scheme by discretizing the spatial domain $\mathbb{R}$ into cells $I_j := [x_{j-1/2}, x_{j+1/2})$, $j \in \mathbb{Z}$, where $x_k = k\Delta x$ for $k = 0, \pm 1/2, \pm 1, \pm 3/2, \ldots$. Similarly, the time interval $(0, T)$ is discretized via $t_n = n\Delta t$ for $n = 0, \ldots, N$, where $N = \lfloor T/\Delta t \rfloor + 1$, which results in the time strips $I^n := [t_n, t_{n+1})$, $n = 0, \ldots, N-1$. Here $\Delta x > 0$ and $\Delta t > 0$ denote the spatial and temporal discretization parameters, respectively. These parameters are chosen so that the following CFL condition holds:

$$\lambda \max_{u \in [0,1], x \in \mathbb{R}} \big| f_u\big(\boldsymbol{\gamma}(x), u\big) \big| + \lambda \max_{x \in \mathbb{R}} \gamma^3(x) \le \frac{1}{2}, \qquad \lambda := \frac{\Delta t}{\Delta x}. \tag{4.1}$$

When sending $\Delta \downarrow 0$ we will do so with the ratio λ kept constant.

We propose a scheme that is a direct modification of the scheme described in [10]. Letting U_j^n denote our approximation to $u(x_j, t^n)$, the marching formula for our new scheme is

$$U_j^{n+1} = U_j^n - \lambda \Delta_- h\big(\boldsymbol{\gamma}_{j+1/2}, U_{j+1}^n, U_j^n\big) + \lambda \gamma_j^3 \, \Delta_+ U_j^n. \tag{4.2}$$

Here $\boldsymbol{\gamma}_{j+1/2} = \boldsymbol{\gamma}(x_{j+1/2}-)$, and $\gamma_j^3 := \gamma^3(x_j-)$. The main difference between (4.2) and the one defined [10] is the term $\lambda \gamma_j^3 \, \Delta_+ U_j^n$ that has been added to incorporate the sink feature of the model. The use of the forward difference Δ_+ in this new sink term is deliberate; we bias this difference to preserve the upwind nature of the scheme. Here we are explicitly using the assumption that $\gamma^3(x) \geq 0$.

The numerical flux $h(\boldsymbol{\gamma}, v, u)$ appearing in (4.2) is the Engquist-Osher (EO henceforth) numerical flux [25]

$$h(\boldsymbol{\gamma}, v, u) := \frac{1}{2}\big(f(\boldsymbol{\gamma}, u) + f(\boldsymbol{\gamma}, v)\big) - \frac{1}{2}\int_u^v |f_u(\boldsymbol{\gamma}, w)| \, dw. \tag{4.3}$$

To define an approximate solution not just at the mesh points, but on all of Π_T, we introduce

$$u^\Delta(x,t) := \sum_{n=0}^{N} \sum_{j \in \mathbb{Z}} \chi_j^n(x,t) U_j^n, \tag{4.4}$$

where χ_j^n is the indicator for the rectangle $I_j \times I^n$.

Although the scheme is not conservative, several important properties of monotonicity are preserved. The following lemma is adapted from Lemma 3.1 of [10].

Lemma 4.1. *The computed solution U_j^n belongs to the interval $[0,1]$. Moreover, the difference scheme (4.2) is monotone.*

Proof. The partial derivatives of U_j^{n+1} with respect to the conserved variables are

$$\frac{\partial U_j^{n+1}}{\partial U_{j+1}^n} = -\lambda f_u^-\big(\boldsymbol{\gamma}_{j+1/2}, U_{j+1}^n\big) + \lambda \gamma_j^3 \geq 0, \quad \frac{\partial U_j^{n+1}}{\partial U_{j-1}^n} = \lambda f_u^+\big(\boldsymbol{\gamma}_{j-1/2}, U_{j-1}^n\big) \geq 0,$$

$$\frac{\partial U_j^{n+1}}{\partial U_j^n} = 1 + \lambda f_u^-\big(\boldsymbol{\gamma}_{j-1/2}, U_j^n\big) - \lambda f_u^+\big(\boldsymbol{\gamma}_{j+1/2}, U_j^n\big) - \lambda \gamma_j^3.$$

Thus U_j^{n+1} is a non-decreasing function of the conserved variables at the lower time level if

$$1 + \lambda f_u^-\big(\boldsymbol{\gamma}_{j-1/2}, U_j^n\big) - \lambda f_u^+\big(\boldsymbol{\gamma}_{j+1/2}, U_j^n\big) - \lambda \gamma_j^3 \geq 0.$$

This will hold if $U_j^n \in [0,1]$ for all j and the CFL condition (4.1) is satisfied. The rest of the proof is similar to the proof of Lemma 3.1 of [10], and is omitted. □

Next we establish a fundamental time-continuity estimate.

Lemma 4.2. *There exists a constant C, independent of Δ and n, such that*

$$\Delta x \sum_{j \in \mathbb{Z}} \big|U_j^{n+1} - U_j^n\big| \leq \Delta x \sum_{j \in \mathbb{Z}} \big|U_j^1 - U_j^0\big| \leq C \Delta t. \tag{4.5}$$

Proof. Starting from the marching formula (4.2), we can express the time differences as follows:

$$\begin{aligned} U_j^{n+1} - U_j^n = U_j^n - U_j^{n-1} &- \lambda \Delta_- \big[h\big(\boldsymbol{\gamma}_{j+1/2}, U_{j+1}^n, U_j^n\big) - h\big(\boldsymbol{\gamma}_{j+1/2}, U_{j+1}^{n-1}, U_j^{n-1}\big)\big] \\ &+ \lambda \gamma_j^3 \Delta_+ U_j^n - \lambda \gamma_j^3 \Delta_+ U_j^{n-1} \end{aligned}$$

$$
\begin{aligned}
&= \big(1 - \lambda C_{j+1/2}^{n-1/2} + \lambda B_{j-1/2}^{n-1/2} - \lambda\gamma_j^3\big)\big(U_j^n - U_j^{n-1}\big) \\
&\quad - \lambda B_{j+1/2}^{n-1/2}\big(U_{j+1}^n - U_{j+1}^{n-1}\big) + \lambda C_{j-1/2}^{n-1/2}\big(U_{j-1}^n - U_{j-1}^{n-1}\big) \\
&\quad + \lambda\gamma_j^3\big(U_{j+1}^n - U_{j+1}^{n-1}\big),
\end{aligned}
$$

where we define

$$
\begin{aligned}
B_{j+1/2}^{n-1/2} &:= \int_0^1 f_u^-\big(\boldsymbol{\gamma}_{j+1/2}, \theta U_{j+1}^n + (1-\theta)U_{j+1}^{n-1}\big)\, d\theta \le 0, \\
C_{j+1/2}^{n-1/2} &:= \int_0^1 f_u^+\big(\boldsymbol{\gamma}_{j+1/2}, \theta U_j^n + (1-\theta)U_j^{n-1}\big)\, d\theta \ge 0.
\end{aligned}
$$

Due to the CFL condition (4.1),

$$
1 - \lambda C_{j+1/2}^{n-1/2} + \lambda B_{j-1/2}^{n-1/2} - \lambda\gamma_j^3 \ge 0. \tag{4.6}
$$

Thus, we conclude that

$$
\begin{aligned}
\big|U_j^{n+1} - U_j^n\big| &\le \big(1 - \lambda C_{j+1/2}^{n-1/2} + \lambda B_{j-1/2}^{n-1/2} - \lambda\gamma_j^3\big)\big|U_j^n - U_j^{n-1}\big| \\
&\quad - \lambda B_{j+1/2}^{n-1/2}\big|U_{j+1}^n - U_{j+1}^{n-1}\big| + \lambda C_{j-1/2}^{n-1/2}\big|U_{j-1}^n - U_{j-1}^{n-1}\big| \\
&\quad + \lambda\gamma_j^3\big|U_{j+1}^n - U_{j+1}^{n-1}\big| \\
&\le \big(1 - \lambda C_{j+1/2}^{n-1/2} + \lambda B_{j-1/2}^{n-1/2} - \lambda\gamma_j^3\big)\big|U_j^n - U_j^{n-1}\big| \\
&\quad - \lambda B_{j+1/2}^{n-1/2}\big|U_{j+1}^n - U_{j+1}^{n-1}\big| + \lambda C_{j-1/2}^{n-1/2}\big|U_{j-1}^n - U_{j-1}^{n-1}\big| \\
&\quad + \lambda\gamma_{j+1}^3\big|U_{j+1}^n - U_{j+1}^{n-1}\big|.
\end{aligned} \tag{4.7}
$$

Here we have used the fact that $x \mapsto \gamma^3(x)$ in non-decreasing when replacing γ_j^3 by γ_{j+1}^3. Summing this inequality over j and multiplying by Δx gives

$$
\Delta x \sum_{j\in\mathbb{Z}} \big|U_j^{n+1} - U_j^n\big| \le \Delta x \sum_{j\in\mathbb{Z}} \big|U_j^n - U_j^{n-1}\big|.
$$

Applying this last inequality inductively, we arrive at

$$
\Delta x \sum_{j\in\mathbb{Z}} \big|U_j^{n+1} - U_j^n\big| \le \Delta x \sum_{j\in\mathbb{Z}} \big|U_j^1 - U_j^0\big|.
$$

The rest of the proof is similar to the proof of Lemma 3.2 of [10] and is omitted. □

Lemmas 4.1 and 4.2 provide several important stability properties of our new difference scheme. We will not pursue the analysis for the full model (2.9), but focus on the reduced problem described in Section 2.3.

5. Convergence to an entropy solution for the reduced problem

In this section we focus our attention on the reduced problem (2.10)–(2.12), which is described in Section 2.3. The goal is to prove the existence of an entropy solution by establishing the convergence of the finite difference scheme from the previous section (as applies to the reduced problem). Later on we remark that by combining this convergence analysis with the one found in [10] we can provide an existence result for the full model.

We can write the scheme for this reduced problem as

$$
U_j^{n+1} = U_j^n - \lambda\Delta_- h(U_{j+1}^n, U_j^n) + \lambda\gamma_j\Delta_+ U_j^n. \tag{5.1}
$$

Here we are abusing the notation slightly by continuing to use the symbol h for the numerical flux, i.e.

$$h(v,u) = \frac{1}{2}\big(\varphi(v)+\varphi(u)\big) - \frac{1}{2}\int_u^v |\varphi'(w)|\, dw.$$

The appropriate CFL condition for our reduced problem is

$$\lambda \max_{u\in[0,1],x\in\mathbb{R}} |\varphi'(u)| + \lambda \max_{x\in\mathbb{R}} \gamma(x) \le \frac{1}{2}, \qquad \lambda := \frac{\Delta t}{\Delta x}. \tag{5.2}$$

In what follows, we utilize the incremental form

$$U_j^{n+1} = U_j^n + C_{j+1/2}^n \Delta_+ U_j^n - D_{j-1/2}^n \Delta_- U_j^n \tag{5.3}$$

of the scheme (5.1), where

$$C_{j+1/2}^n = \lambda\left(\frac{\varphi(U_j^n) - h(U_{j+1}^n, U_j^n)}{\Delta_+ U_j^n} + \gamma_j\right), \quad D_{j-1/2}^n = \lambda \frac{\varphi(U_j^n) - h(U_j^n, U_{j-1}^n)}{\Delta_- U_j^n}.$$

Using the monotonicity of the numerical flux h, that $\gamma_j \ge 0$, and the CFL condition (5.2), one can easily check that

$$C_{j+1/2}^n \ge 0, \quad D_{j+1/2}^n \ge 0, \quad C_{j+1/2}^n + D_{j+1/2}^n \le 1. \tag{5.4}$$

Lemmas 4.1 and 4.2 remain valid in this setting, and need not be repeated. In order to establish compactness, we will also need a spatial variation bound, which is provided by the following lemma. Let $V_a^b(z)$ denote the total variation of the function $x \mapsto z(x)$ over the interval $[a,b]$.

Lemma 5.1. *For any interval $[a,b]$, and any $t \in [0,T]$ we have a spatial variation bound of the form*

$$V_a^b\big(u^\Delta(\cdot,t)\big) \le C, \tag{5.5}$$

where C is independent of Δ and t for $t \in [0,T]$.

Proof. Due to our time continuity estimate (4.5), there is a constant K such that

$$\Delta x \sum_{j\in\mathbb{Z}} \sum_{n=0}^{N} \big|U_j^{n+1} - U_j^n\big| \le K. \tag{5.6}$$

Fix $r > 0$, and without loss of generality, assume that $r > \Delta x$ for all mesh sizes Δx of interest. Let

$$\mathcal{A} := \mathcal{A}(\Delta) := \{j | x_j \in [a - r - \Delta x, a]\}, \quad \mathcal{B} := \mathcal{B}(\Delta) := \{j | x_j \in [b, b + r + \Delta x]\},$$

and observe that $|\mathcal{A}|\Delta x \ge r$, $|\mathcal{B}|\Delta x \ge r$. It is then clear that

$$\Delta x \sum_{j\in\mathcal{A}} \sum_{n=0}^{N} \big|U_j^{n+1} - U_j^n\big| \le K, \quad \Delta x \sum_{j\in\mathcal{B}} \sum_{n=0}^{N} \big|U_j^{n+1} - U_j^n\big| \le K. \tag{5.7}$$

We can choose $j_a = j_a(\Delta)$, $j_b = j_b(\Delta)$ with $j_a \in \mathcal{A}$, $j_{b+1} \in \mathcal{B}$ such that

$$\sum_{n=0}^{N} \big|U_{j_a}^{n+1} - U_{j_a}^n\big| = \min_{j\in\mathcal{A}} \sum_{n=0}^{N} \big|U_j^{n+1} - U_j^n\big|,$$

$$\sum_{n=0}^{N} \big|U_{j_b+1}^{n+1} - U_{j_b+1}^n\big| = \min_{j\in\mathcal{B}} \sum_{n=0}^{N} \big|U_j^{n+1} - U_j^n\big|.$$

It follows from (5.7) that

$$\begin{aligned}\sum_{n=0}^{N}\left|U_{j_a}^{n+1}-U_{j_a}^{n}\right| &\le \frac{K}{|\mathcal{A}|\Delta x}\le\frac{K}{r},\\ \sum_{n=0}^{N}\left|U_{j_b+1}^{n+1}-U_{j_b+1}^{n}\right| &\le \frac{K}{|\mathcal{B}|\Delta x}\le\frac{K}{r}.\end{aligned}\tag{5.8}$$

The incremental form (5.3) implies that the differences evolve according to

$$\begin{aligned}\Delta_+U_j^{n+1} = \Delta_+U_j^n &+ C_{j+3/2}^n\Delta_+U_{j+1}^n - C_{j+1/2}^n\Delta_+U_j^n\\ &- D_{j+1/2}^n\Delta_+U_j^n + D_{j-1/2}^n\Delta_-U_j^n.\end{aligned}\tag{5.9}$$

Note that when $j=j_a$, we can write (5.9) as

$$\Delta_+U_{j_a}^{n+1} = \Delta_+U_{j_a}^n + C_{j_a+3/2}^n\Delta_+U_{j_a+1}^n - D_{j_a+1/2}^n\Delta_+U_{j_a}^n - \left(U_{j_a}^{n+1}-U_{j_a}^n\right).\tag{5.10}$$

Similarly, when $j=j_b$, (5.9) takes the form

$$\Delta_+U_{j_b}^{n+1} = \Delta_+U_{j_b}^n - C_{j_b+1/2}^n\Delta_+U_{j_b}^n + D_{j_b-1/2}^n\Delta_-U_{j_b}^n + \left(U_{j_b+1}^{n+1}-U_{j_b+1}^n\right).\tag{5.11}$$

Taking absolute values and summing over j in (5.9), we use the properties (5.4) to proceed as in the proof of Harten's lemma (Lemma 2.2 of [31]). To deal with the boundary contributions, we use (5.10) and (5.11). This calculation yields

$$\begin{aligned}\sum_{j=j_a}^{j_b}\left|\Delta_+U_j^{n+1}\right| \le{}& \left(1-D_{j_a+1/2}^n\right)\left|\Delta_+U_{j_a}^n\right| + C_{j_a+3/2}^n\left|\Delta_+U_{j_a+1}^n\right| + \left|U_{j_a}^{n+1}-U_{j_a}^n\right|\\ &+\sum_{j=j_a+1}^{j_b-1}\left(1-C_{j+1/2}^n-D_{j+1/2}^n\right)\left|\Delta_+U_j^n\right|\\ &+\sum_{j=j_a+1}^{j_b-1}C_{j+3/2}^n\left|\Delta_+U_{j+1}^n\right| + \sum_{j=j_a+1}^{j_b-1}D_{j-1/2}^n\left|\Delta_-U_j^n\right|\\ &+\left(1-C_{j_b+1/2}\right)\left|\Delta_+U_{j_b}^n\right| + D_{j_b-1/2}^n\left|\Delta_-U_{j_b}^n\right| + \left|U_{j_b+1}^{n+1}-U_{j_b+1}^n\right|\\ \le{}& \sum_{j=j_a}^{j_b}\left|\Delta_+U_j^n\right| + \left|U_{j_a}^{n+1}-U_{j_a}^n\right| + \left|U_{j_b+1}^{n+1}-U_{j_b+1}^n\right|.\end{aligned}$$

Proceeding by induction, and then using (5.8), we find that for $1\le n\le N$

$$\begin{aligned}\sum_{j=j_a}^{j_b}\left|\Delta_+U_j^n\right| &\le \sum_{j=j_a}^{j_b}\left|\Delta_+U_j^0\right| + \sum_{\nu=1}^{n}\left(\left|U_{j_a}^{\nu}-U_{j_a}^{\nu-1}\right| + \left|U_{j_b+1}^{\nu}-U_{j_b+1}^{\nu-1}\right|\right)\\ &\le \sum_{j=j_a}^{j_b}\left|\Delta_+U_j^0\right| + \frac{2K}{r}.\end{aligned}$$

The proof is completed with the observation that $[a,b]\subseteq[x_{j_a},x_{j_{b+1}}]$, along with the assumption that u_0 has bounded variation. □

Remark 5.1. It is clear from the incremental form (5.3) that we could have simply used Harten's lemma [31] in its unmodified form to conclude that the scheme is Total Variation Diminishing (TVD), thus giving a direct proof of a global spatial variation bound. We chose this somewhat more involved proof because within the context of

the more complete model (2.9), it would not be possible to use Harten's Lemma. More specifically, the discontinuities in the spatially varying coefficient $\boldsymbol{\gamma}$ preclude the use of the elementary TVD type arguments like Harten's lemma. We would only have the time continuity estimate (Lemma 4.2) from which to derive a spatial variation bound, and this more local variation bound would have to suffice. Finally, note that the local BV approach appearing here could be applied to simplify the compactness proof for the model appearing in [10]. In the situation studied there, the sink term was not present but the flux had several spatial discontinuities. The singular mapping approach, which by now is standard for such conservation laws, was used to establish compactness. The singular mapping approach becomes rather complicated when the flux has multiple extrema, as in the case of the clarifier-thickener model. One could instead use the approach of Lemma 5.1 to derive a variation bound for any open subset of $\mathbb{R}$ not containing any of the jumps in the flux, and then invoke a standard diagonal argument to achieve compactness on all of $\mathbb{R}$. We will not pursue this further here, but see the forthcoming paper [14].

In what follows, we will employ the following regularizations of the function $\gamma(x)$.

$$\overline{\gamma}^\epsilon(x) := \begin{cases} 0 & \text{for } x \le -\epsilon, \\ ((x+\epsilon)/\epsilon)\gamma_+ & \text{for } -\epsilon \le x \le 0, \\ \gamma_+ & \text{for } x \ge 0, \end{cases}$$

$$\underline{\gamma}^\epsilon(x) := \begin{cases} 0 & \text{for } x \le 0, \\ (x/\epsilon)\gamma_+ & \text{for } 0 \le x \le \epsilon, \\ \gamma_+ & \text{for } x \ge \epsilon. \end{cases}$$

Observe that $\underline{\gamma}^\epsilon(x) \le \gamma(x) \le \overline{\gamma}^\epsilon(x)$ for all $x \in \mathbb{R}$. When discretizing $\underline{\gamma}^\epsilon$ and $\overline{\gamma}^\epsilon$, we do so in the same manner as γ, thus preserving the ordering $\underline{\gamma}^\epsilon_j \le \gamma_j \le \overline{\gamma}^\epsilon_j$.

One more preliminary issue before we discuss entropy conditions is the existence of traces along the line $x = 0$, $t \in [0,T]$. Our spatial BV bounds carry over to the limit solution u, guaranteeing that we have limits from both the left and right, denoted $u_-(t), u_+(t)$ or simply u_-, u_+, for a.e $t \in [0,T]$.

Lemma 5.2. *Any (subsequential) limit u of the scheme* (5.1) *satisfies the entropy conditions* (3.1)–(3.6).

Proof. The proof of the Kružkov-type entropy inequalities (3.1), (3.2) is standard [17], and is omitted.

We now turn to the proof of (3.3). The following discrete entropy inequality holds for any $c \in \mathbb{R}$; this follows from the monotonicity property of the scheme:

$$U_j^{n+1} \vee c \le U_j^n \vee c - \lambda \Delta_+ h\left(U_j^n \vee c, U_{j-1}^n \vee c\right) + \lambda \gamma_j \Delta_+ \left(U_j^n \vee c\right). \tag{5.12}$$

Now let

$$V_j^n := \begin{cases} c & \text{for } j \le 0, \\ U_j^n \vee c & \text{for } j > 0, \end{cases} \qquad v(x,t) := \begin{cases} c & \text{for } x < 0, \\ u(x,t) \vee c & \text{for } x > 0. \end{cases}$$

Note that

$$\Delta_+ V_0^n = U_1^n \vee c - c \ge 0. \tag{5.13}$$

Since $\gamma_j = 0$ for $j \le 0$, and $\Delta_+ V_j^n = \Delta_+(U_j^n \vee c)$ for $j > 0$, we can replace inequality (5.12) by

$$U_j^{n+1} \vee c \le U_j^n \vee c - \lambda \Delta_+ h\left(U_j^n \vee c, U_{j-1}^n \vee c\right) + \lambda \gamma_j \Delta_+ V_j^n. \tag{5.14}$$

Since $\overline{\gamma}_j^\epsilon \ge \gamma_j = 0$ for $j \le 0$ and $\overline{\gamma}_j^\epsilon = \gamma_j = \gamma_+$ for $j > 0$, in view of (5.13) we can replace inequality (5.14) by

$$U_j^{n+1} \vee c \le U_j^n \vee c - \lambda \Delta_+ h\left(U_j^n \vee c, U_{j-1}^n \vee c\right) + \lambda \overline{\gamma}_j^\epsilon \Delta_+ V_j^n. \tag{5.15}$$

Employing the identity

$$A_j \Delta_+ B_j = \Delta_+ \left(A_j B_j\right) - B_{j+1} \Delta_+ A_j, \tag{5.16}$$

we can rewrite (5.15) in the form

$$U_j^{n+1} \vee c \le U_j^n \vee c - \lambda \Delta_+ \big(h\left(U_j^n \vee c, U_{j-1}^n \vee c\right) - \overline{\gamma}_j^\epsilon V_j^n\big) - \lambda V_{j+1}^n \Delta_+ \overline{\gamma}_j^\epsilon. \tag{5.17}$$

Let $0 \le \psi \in \mathcal{D}(\Pi_T)$, and $\psi_j^n = \psi(x_j, t^n)$. Proceeding as in the proof of the Lax-Wendroff theorem, we move all of the terms in (5.17) to the left-hand side of the inequality, multiply by $\psi_j^n \, \Delta x$, and sum over $j \in \mathbb{Z}$, $n \ge 0$, and finally sum by parts to get

$$\begin{aligned} &\Delta x \Delta t \sum_{j \in \mathbb{Z}} \sum_{n \ge 0} \left(U_j^n \vee c\right) \frac{\psi_j^{n+1} - \psi_j^n}{\Delta t} \\ &\quad + \Delta x \Delta t \sum_{j \in \mathbb{Z}} \sum_{n \ge 0} \left[h\left(U_j^n \vee c, U_{j-1}^n \vee c\right) - \overline{\gamma}_j^\epsilon V_j^n\right] \frac{\Delta_+ \psi_j^n}{\Delta x} \\ &\quad - \Delta x \Delta t \sum_{j \in \mathbb{Z}} \sum_{n \ge 0} \frac{\Delta_+ \overline{\gamma}_j^\epsilon}{\Delta x} V_{j+1}^n \psi_j^n \ge 0. \end{aligned} \tag{5.18}$$

When $\Delta \downarrow 0$, the bounded convergence theorem yields

$$\iint_{\Pi_T} \Big((u \vee c)\psi_t + (\varphi(u \vee c) - \overline{\gamma}^\epsilon(x) v)\, \psi_x\Big)\, dx\, dt - \iint_{\Pi_T} (\overline{\gamma}^\epsilon)'(x)\, v\, \psi\, dx\, dt \ge 0. \tag{5.19}$$

With the observation that

$$(\overline{\gamma}^\epsilon)'(x) = \begin{cases} \gamma_+/\epsilon & \text{for } x \in (-\epsilon, 0), \\ 0 & \text{for } x \notin (-\epsilon, 0), \end{cases}$$

when $\epsilon \downarrow 0$ we obtain

$$\iint_{\Pi_T} (\overline{\gamma}^\epsilon)'(x)\, v\, \psi\, dx\, dt \to \gamma_+ c \int_0^T \psi(0,t)\, dt.$$

Combining this with an application of the bounded convergence theorem, when $\epsilon \downarrow 0$, (5.19) yields the inequality

$$\iint_{\Pi_T} \Big((u \vee c)\psi_t + \big(\varphi(u \vee c) - \gamma(x) v\big)\psi_x\Big)\, dx\, dt - \gamma_+ c \int_0^T \psi(0,t)\, dt \ge 0. \tag{5.20}$$

By applying a standard test function argument to (5.20), we find that for a.e. $t \in (0,T)$,

$$\varphi(u_-(t) \vee c) - \gamma_- c - \big(\varphi(u_+(t) \vee c) - \gamma_+ (u_+(t) \vee c)\big) - \gamma_+ c \ge 0.$$

Recalling that $\gamma_- = 0$, $u_- \le c \le u_+$, dropping the dependence on t, and rearranging, this inequality becomes

$$\varphi(u_+) - \varphi(c) \le \gamma_+(u_+ - c),$$

and the proof of (3.3) is complete.

For the proof of (3.4) we use the monotonicity of the scheme to derive the discrete entropy inequality

$$U_j^{n+1} \wedge c \ge U_j^n \wedge c - \lambda \Delta_+ h\left(U_j^n \wedge c, U_{j-1}^n \wedge c\right) + \lambda \gamma_j \Delta_+ \left(U_j^n \wedge c\right). \tag{5.21}$$

Let

$$W_j^n := \begin{cases} c & \text{for } j \le 0, \\ U_j^n \wedge c & \text{for } j > 0, \end{cases}, \qquad w(x,t) := \begin{cases} c & \text{for } x < 0, \\ u(x,t) \wedge c & \text{for } x > 0. \end{cases}$$

Observing that

$$\Delta_+(U_0^n \wedge c) = U_1^n \wedge c - U_0^n \wedge c \ge \Delta_+ W_0^n = U_1^n \wedge c - c \le 0, \tag{5.22}$$

we find that the following inequality holds:

$$U_j^{n+1} \wedge c \ge U_j^n \wedge c - \lambda \Delta_+ h\left(U_j^n \wedge c, U_{j-1}^n \wedge c\right) + \lambda \gamma_j \Delta_+ W_j^n. \tag{5.23}$$

Using $0 \le \gamma_j \le \overline{\gamma}_j^\epsilon$ and $\Delta_+ W_0^n \le 0$, we also have

$$U_j^{n+1} \wedge c \ge U_j^n \wedge c - \lambda \Delta_+ h\left(U_j^n \wedge c, U_{j-1}^n \wedge c\right) + \lambda \overline{\gamma}_j^\epsilon \Delta_+ W_j^n. \tag{5.24}$$

Proceeding as in the proof of (3.3), we find that

$$\iint_{\Pi_T} \Big((u \wedge c)\psi_t + \big(\varphi(u \wedge c) - \overline{\gamma}^\epsilon(x) w\big)\psi_x \Big)\, dx\, dt - \iint_{\Pi_T} (\overline{\gamma}^\epsilon)'(x)\, w\, \psi\, dx\, dt \le 0,$$

from which it follows that

$$\varphi(u_-(t) \wedge c) - \gamma_- c - \big(\varphi(u_+(t) \wedge c) - \gamma_+(u_+(t) \wedge c)\big) - \gamma_+ c \le 0,$$

and this holds for a.e. $t \in [0,T]$. Recalling that $\gamma_- = 0$, and then observing that the terms involving $\gamma_+(u_+(t) \wedge c)$ and $\gamma_+ c$ cancel, the proof of (3.4) is complete.

For the proof of (3.6), we start from the discrete entropy inequality (5.12), and then apply the identity (5.16) to get

$$\begin{aligned} U_j^{n+1} \vee c \le U_j^n \vee c - \lambda \Delta_+ \big(& h\left(U_j^n \vee c, U_{j-1}^n \vee c\right) - \gamma_j (U_j^n \vee c)\big) \\ & - \lambda (U_{j+1}^n \vee c) \Delta_+ \gamma_j. \end{aligned} \tag{5.25}$$

We then define

$$\tilde{V}_j^n := \begin{cases} U_j^n \vee c & \text{for } j \le 0, \\ c & \text{for } j > 0, \end{cases} \qquad \tilde{v}(x,t) := \begin{cases} u(x,t) \vee c & \text{for } x < 0, \\ c & \text{for } x > 0, \end{cases}$$

and observe that it is possible to replace the inequality (5.25) by

$$U_j^{n+1} \vee c \le U_j^n \vee c - \lambda \Delta_+ \big(h\left(U_j^n \vee c, U_{j-1}^n \vee c\right) - \gamma_j (U_j^n \vee c)\big) - \lambda \tilde{V}_{j+1}^n \Delta_+ \gamma_j. \tag{5.26}$$

More specifically, this inequality holds because $\Delta_+ \gamma_j = 0$, except at $j = 0$, and $U_1^n \vee c \ge \tilde{V}_1 = c$. Another application of the identity (5.16) yields

$$\begin{aligned} U_j^{n+1} \vee c \le U_j^n \vee c - \lambda \Delta_+ \big(& h\left(U_j^n \vee c, U_{j-1}^n \vee c\right) - \gamma_j (U_j^n \vee c) + \gamma_j \tilde{V}_j^n \big) \\ & + \lambda \gamma_j \Delta_+ \tilde{V}_j^n. \end{aligned} \tag{5.27}$$

Since $\Delta_+\tilde{V}_j^n = 0$ for $j > 0$, $\Delta_+\tilde{V}_0^n \le 0$, $\underline{\gamma}_j^\epsilon = \gamma_j$ for $j < 0$, and $\underline{\gamma}_j^\epsilon \le \gamma_j$ for $j \ge 0$, we can replace (5.27) by

(5.28)
$$U_j^{n+1} \vee c \le U_j^n \vee c - \lambda\Delta_+\big(h\left(U_j^n \vee c, U_{j-1}^n \vee c\right) - \gamma_j(U_j^n \vee c) + \gamma_j\tilde{V}_j^n\big) + \lambda\underline{\gamma}_j^\epsilon\Delta_+\tilde{V}_j^n.$$

A final application of (5.16) results in

(5.29)
$$U_j^{n+1} \vee c \le U_j^n \vee c - \lambda\Delta_+\big(h\left(U_j^n \vee c, U_{j-1}^n \vee c\right) - \gamma_j(U_j^n \vee c) + (\gamma_j - \underline{\gamma}_j^\epsilon)\tilde{V}_j^n\big) - \lambda\tilde{V}_{j+1}^n\Delta_+\underline{\gamma}_j^\epsilon.$$

The rest of the proof of (3.6) is similar to the proofs of (3.3) and (3.4), and so we omit the details.

The proof of (3.5) is similar to the proof of (3.6), the main difference being that one starts from the discrete entropy inequality (5.21) and uses the modified functions

$$\tilde{W}_j^n := \begin{cases} U_j^n \wedge c & \text{for } j \le 0, \\ c & \text{for } j > 0, \end{cases}, \qquad \tilde{w}(x,t) := \begin{cases} u(x,t) \wedge c & \text{for } x < 0, \\ c & \text{for } x > 0. \end{cases}$$

We omit the details. □

We can now state and prove our main theorem.

Theorem 5.1. *As $\Delta \downarrow 0$, the approximations u^Δ generated by the scheme* (5.1) *converge in $L^1(\Pi_T)$ and a.e. in Π_T to the unique entropy solution u of the initial value problem* (2.10)–(2.12)*.*

Proof. Recalling the proof of Lemma 5.1, we see that the constant C appearing in our spatial variation bound (5.5) is independent of the interval $[a, b]$. Letting $a \to -\infty$, $b \to \infty$, we obtain a uniform spatial variation bound over all of $\mathbb{R}$. Thus, we have an L^∞ bound (Lemma 4.1), a time continuity bound (Lemma 4.2), and a spatial variation bound (Lemma 5.1). In addition, it is a straightforward exercise using the time continuity bound provided by Lemma 4.2 to derive a bound for the approximations u^Δ in the $L^1(\Pi_T)$ norm. Moreover, these bounds are independent of Δ, for $(x,t) \in \Pi_T$. It follows from standard compactness arguments that there is a subsequential limit, converging in $L^1(\Pi_T)$, and a.e. in Π_T, which we will denote u. A proof of (3.7), i.e., that the initial values are assumed in the strong L^1 sense is standard and is thus omitted. The proof is completed with an application of our Lemma 5.2, which guarantees that the subsequential limit u is an entropy solution. By our uniqueness result (Theorem 3.1), the entire sequence converges to u. □

Theorem 5.1 shows that there exists a unique entropy solution to the initial value problem (2.10)–(2.12), i.e., that this problem is well-posed.

Remark 5.2. Our ultimate interest is the more complicated scheme (4.2) which we use to construct approximate solutions of the full model. We have focused on the reduced model and its associated scheme in order to highlight the aspects of the problem that are more or less unique to the sink portion of the model. We also wished to avoid repeating those portions of the analysis that we have documented in [10]. By combining the definition of entropy solution and the results of the present paper with those of [10], it is straightforward to conclude that the version of Theorem 5.1 that applies to the full problem is also true. Specifically, using the

more complicated scheme (4.2), we also have convergence to the unique entropy solution of the full problem.

6. Variants of the difference scheme

The scheme described herein for the full problem has the slight inconvenience that in order to determine the Engquist-Osher flux function, one has to determine the extrema of the composite flux function $q(u-u_{\mathrm{F}})+b(u)$ for $q \in \{q_{\mathrm{L}}, \tilde{q}_{\mathrm{R}}\}$ numerically. This can be avoided if we determine the Engquist-Osher flux function for the function $b(u)$ only, and discretize the linear portion $q(u-u_{\mathrm{F}})$ by a properly oriented upwind stencil. The resulting scheme, to which we shall refer as "Scheme 1", then reads

$$\begin{aligned} U_j^{n+1} = U_j^n &- \lambda \Delta_- h^1\big(\gamma^1_{j+1/2}, U^n_{j+1}, U^n_j\big) \\ &- \lambda w\big(\gamma^2_{j-1/2}, \gamma^2_{j+1/2}, U^n_{j-1}, U^n_j, U^n_{j+1}\big) + \lambda \gamma^3_j \Delta_+ U^n_j, \end{aligned}$$

where $\gamma^1, \gamma^2, \gamma^3$ are defined in (2.7), (2.8) and the function h^1 is the EO flux applied to the function $\gamma^1 b(u)$, i.e.,

$$h^1(\gamma^1, v, u) = \frac{\gamma^1}{2}\left(b(u) + b(v) - \int_u^v |b'(s)|\, ds\right), \tag{6.1}$$

and the function w arises from determining the EO flux for the linear term $\gamma^2(x)u$, followed by differencing with respect to x, i.e.,

$$w\big(\gamma^2_{j-1/2}, \gamma^2_{j+1/2}, U^n_{j-1}, U^n_j, U^n_{j+1}\big) := \Delta_- \tilde{h}\big(\gamma^2_{j+1/2}, U^n_{j+1} - u_{\mathrm{F}}, U_j - u_{\mathrm{F}}\big),$$

where we define

$$\tilde{h}(\gamma^2, v, u) := \frac{1}{2}\left(\gamma^2(u+v) - \int_u^v \big|\gamma^2(s)\big| ds\right).$$

This yields the upwind formula

$$\begin{aligned} &w\big(\gamma^2_{j-1/2}, \gamma^2_{j+1/2}, U^n_{j-1}, U^n_j, U^n_{j+1}\big) \\ &= \begin{cases} \gamma^2_{j+1/2}\big(U^n_j - u_{\mathrm{F}}\big) - \gamma^2_{j-1/2}\big(U^n_{j-1} - u_{\mathrm{F}}\big) & \text{if } \gamma^2_{j-1/2} \geq 0 \text{ and } \gamma^2_{j+1/2} \geq 0, \\ \gamma^2_{j+1/2}\big(U^n_{j+1} - u_{\mathrm{F}}\big) - \gamma^2_{j-1/2}\big(U^n_j - u_{\mathrm{F}}\big) & \text{if } \gamma^2_{j-1/2} < 0 \text{ and } \gamma^2_{j+1/2} < 0, \\ \big(\gamma^2_{j+1/2} - \gamma^2_{j-1/2}\big)\big(U^n_j - u_{\mathrm{F}}\big) & \text{if } \gamma^2_{j+1/2} \geq 0 \text{ and } \gamma^2_{j-1/2} < 0. \end{cases} \end{aligned}$$

For easy reference, let us refer to the scheme (4.2), (4.3), which is analyzed in this paper, as "Scheme 2". Clearly, Scheme 1 emerges from Scheme 2 by applying a direct upwind linearization, and avoiding the EO formula, for as many terms as possible. As we shall see, the performance of Scheme 1 is much inferior to that of Scheme 2 in terms of numerical viscosity. On the other hand, this observation suggests that an even better scheme can possibly be produced if we replace Scheme 2 by a new scheme, called Scheme 3, if we avoid any explicit linear upwind differences at all, and express the numerical flux on all segments as one EO-flux. Thus, the marching formula for Scheme 3 is

$$U_j^{n+1} = \begin{cases} U^n_j - \lambda \Delta_- h^3\big(\tilde{\boldsymbol{\gamma}}_{j+1/2}, \gamma^3_{j+1/2}, U^n_{j+1}, U^n_j\big) & \text{for } j > 0, \\ U^n_j - \lambda \Delta_- h^2\big(\tilde{\boldsymbol{\gamma}}_{j+1/2}, U^n_{j+1}, U^n_j\big) & \text{for } j \leq 0, \end{cases} \tag{6.2}$$

Case	q	$-\gamma_+$	$u_0(x)$	λ
1	-4.9	-4.3	$0.1\chi_{[-2,2]}(x)$	0.03125
2	-2.8	-2.6	$0.1\chi_{[-1,1]}(x)$	0.04
3	-4.9	0	$0.1\chi_{[-2,-0.4]}(x)$	0.04
4	-4.9	-4.9	$0.1\chi_{[-2,-0.4]}(x)$	0.025

TABLE 1. Parameters for the numerical examples for the reduced problem shown in Figure 3.

Case	q_{L}	q_{D}	q_{R}	u_{F}	λ
5	0.0	-1.0	0.6	0.7	0.05333
6	-0.7	-0.3	0.6	0.7	0.06289
7	-2.25	-2.25	1.35	0.3	0.03922
8	-3.6	-2.25	1.35	0.3	0.03968

TABLE 2. Parameters for the numerical examples for the full model shown in Figure 4.

where we define $\tilde{\boldsymbol{\gamma}} := (\gamma^1, \gamma^2)$ and

$$h^2(\tilde{\boldsymbol{\gamma}}, v, u) := \frac{1}{2}\bigg(f(\tilde{\boldsymbol{\gamma}}, u) + f(\tilde{\boldsymbol{\gamma}}, v) - \int_u^v \big| f_u(\tilde{\boldsymbol{\gamma}}, w) \big| \, dw \bigg),$$

$$h^3(\tilde{\boldsymbol{\gamma}}, \gamma^3, v, u) := \frac{1}{2}\bigg(f(\tilde{\boldsymbol{\gamma}}, u) + f(\tilde{\boldsymbol{\gamma}}, v) - \gamma^3(u+v) - \int_u^v \big| f_u(\tilde{\boldsymbol{\gamma}}, w) - \gamma^3 \big| \, dw \bigg).$$

For the simplified version of Scheme 1 that applies to the reduced problem (2.10)–(2.12), it is possible to prove convergence to an entropy solution by repeating the analysis in Section 5. For Scheme 3, the convergence proof still goes through, but it is not clear that our proof of convergence to an entropy solution (Lemma 5.2) is directly applicable. However, our numerical experiments seem to indicate that approximations generated by Scheme 3 converge to the same (entropy) solutions as provided by Schemes 1 and 2.

7. Numerical results

7.1. **Numerical solutions of the reduced problem.** In the first series of examples, Cases 1 to 4, we consider the reduced problem (2.10)–(2.12). We assume that the function $b(u)$ is given by (1.4) with $v_\infty = 6.75$, $u_{\max} = 1$ and $n = 2$. The plots of Figure 3 correspond to the parameters given in Table 1. The simulations have been made with Scheme 3, $\Delta x = 1/40$, and the values of $\lambda = \Delta t/\Delta x$ indicated in Table 1. Note that the sink term in Case 3 is switched off. This solution of a standard nonlinear conservation law has been included to illustrate the difference to Case 4, where the sink term is included, but all other parameters are the same.

7.2. **Numerical solutions of the full problem.** Next, we consider the full extended clarifier-thickener model (2.6)–(2.9), (2.11). The parameters of four different simulations shown in Figure 4, Cases 5 to 8, are shown in Table 2. In all cases, we start from an initially empty clarifier-thickener unit ($u_0 \equiv 0$), and consider the same function $b(u)$ as for Cases 1 to 4. The simulations have been made with $\Delta x = 1/40$ and the values of λ given in Table 2.

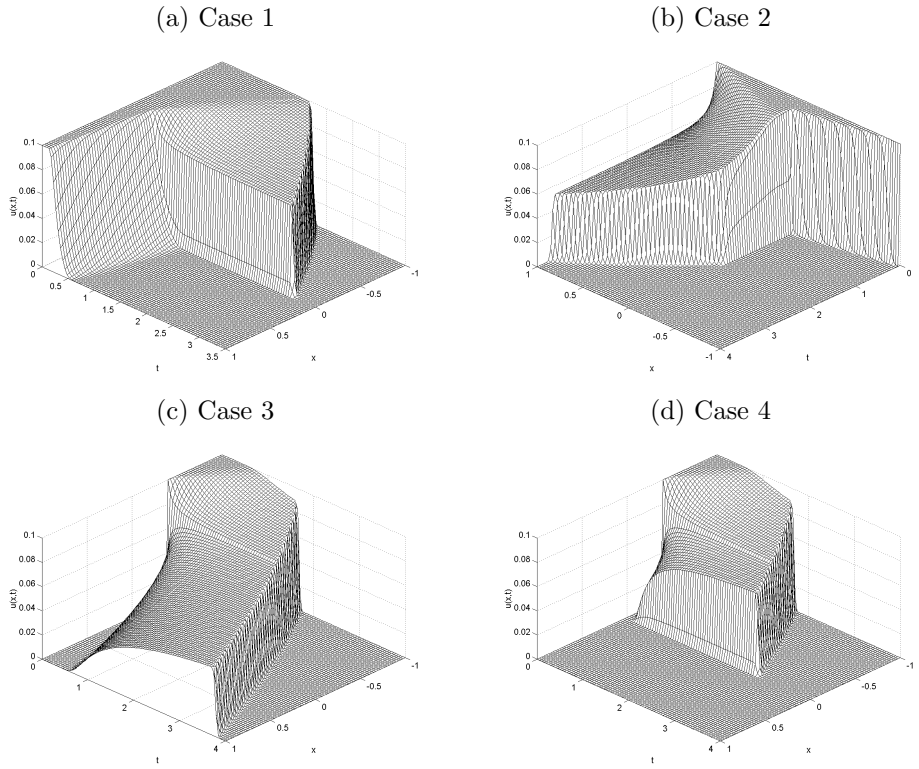

FIGURE 3. Numerical examples with $\Delta x = 0.025$ for the reduced problem.

7.3. **Error study.** We consider first Case 1, which corresponds to the reduced problem. Figure 5 shows the numerical solution produced by Schemes 1, 2 and 3 for $t = 0.5$ and $t = 2$, while Table 3 displays the approximate L^1 error for this case, measured over the interval $[-1, 1]$.

Next, we consider Case 5, which corresponds to the full problem. Figure 6 shows the numerical solution produced by Schemes 1, 2 and 3 for $t = 1$, $t = 2$ and $t = 4$, respectively, while Table 4 displays the approximate L^1 error for this case, measured over the interval $[-2.1, 1.1]$ (so that all flux discontinuities are included). Finally, we present in Figure 7 numerical solutions generated by all three schemes for Case 7 and $t = 0.3$ and $t = 10$. The corresponding approximate L^1 errors are shown in Table 5.

7.4. **Conclusion and discussion.** Figure 3 illustrates that the sink term gives rise to a variety of stationary discontinuities. In fact, the reduced problem models how material whose flow is otherwise governed by the conservation law $u_t + \varphi(u)_x = 0$ is absorbed by a singular sink. In Cases 1 and 4, the sink produces a decreasing step (in the direction of increasing x), while in Case 2, an increasing step is generated. Observe that in Case 2, roughly at $t = 2$, the stationary discontinuity at $x = 0$ ceases to exist, and is followed by a curved shock moving in the direction of $x > 0$.

The parameters in Figure 4 have been chosen in such a way that either the solid material flowing into the clarifier zone is fully absorbed by the singular sink term

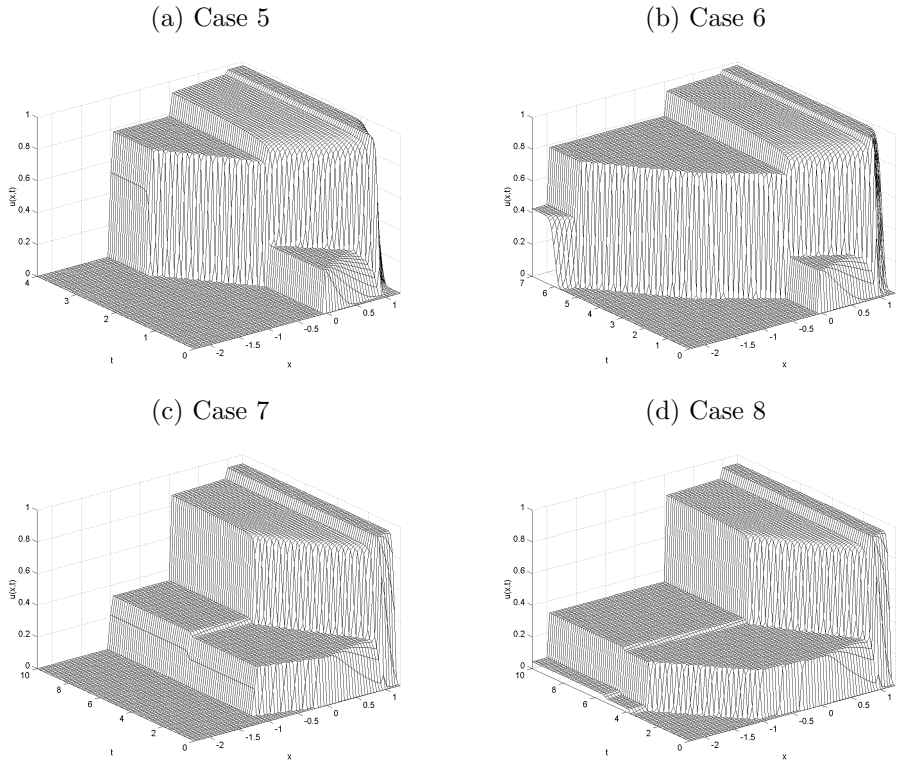

FIGURE 4. Numerical examples with $\Delta x = 0.025$ for the full extended clarifier-thickener model.

(Cases 5 and 7), or material is extracted through the sink without affecting the solution in the clarifier zone (Cases 6 and 8). The absence of a discontinuity across $x = x_{\mathrm{D}} = -1$ in these cases can be made plausible if we look at the associated reduced problem for the parameters given in these cases. For instance, Case 6 corresponds to $q = q_{\mathrm{L}} = -0.7$. We observe in Figure 4 (b) that the solution in the clarification zone after the solids break through the feed level assumes at least a value of 0.78. However, inspecting the shape of $u \mapsto b(u)$ it is easy to see that we have

$$\begin{aligned}
&\sup_{u^+\in[0.78,1]} \max_{u^-\in[0,1]} \frac{\varphi(u^+) - \varphi(u^-)}{u^+ - u^-} \\
&\quad = q + \sup_{u^+\in[0.78,1]} \max_{u^-\in[0,1]} \frac{b(u^+) - b(u^-)}{u^+ - u^-} \\
&\quad \le q + \frac{b(0.78) - b(0)}{0.78} = -0.7 + 6.75 \times 0.22^2 = -0.3733,
\end{aligned}$$

so for this value and $u_+ \ge 0.78$ (in fact, we may choose this lower bound even smaller), the left-hand inequality in jump condition (3.9) is never satisfied. In other words, from an engineering point of view, jump condition (3.9) helps to predict under which flow conditions extracting material from a sink affects the

(a) Case 1, $t = 0.5$, $\Delta x = 1/40$ (b) Case 1, $t = 0.5$, $\Delta x = 1/80$

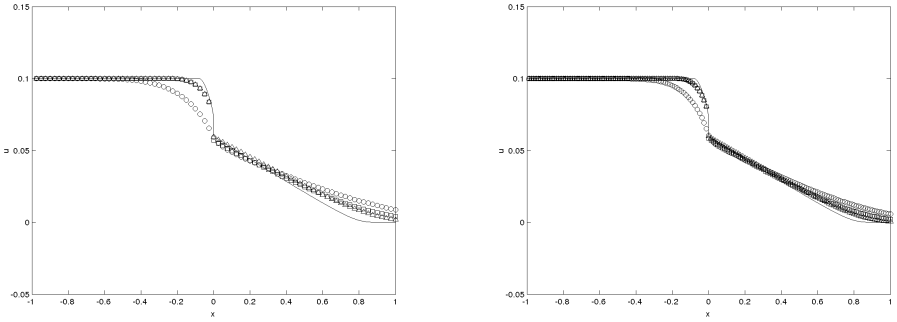

(c) Case 1, $t = 2$, $\Delta x = 1/40$ (d) Case 1, $t = 2$, $\Delta x = 1/80$

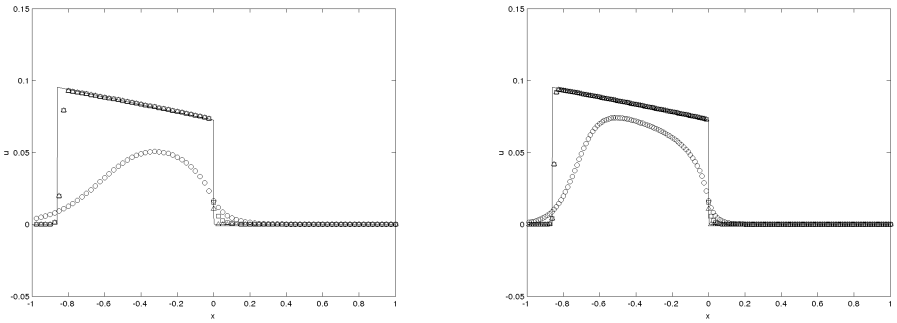

FIGURE 5. Comparison of Scheme 1 (∘), Scheme 2 (□) and Scheme 3 (△) applied to Case 1. The solid line is a reference solution with $\Delta x = 1/1600$.

bulk concentration (i.e., causes a concentration jump) and under which conditions this does not happen (as in our Cases 6 and 8).

Figures 5 to 7 and Tables 3 to 5 illustrate that all schemes converge to the unique entropy solution of the reduced problem or the full extended clarifier-thickener model. However, all these results also show that Scheme 1, though it has the convenience of being easy to implement, suffers from excessive numerical viscosity, which becomes apparent in smearing of transient shocks travelling at nonzero speed (for example, near $x = 0.5$ in Figures 6 (a) and (b)) and the formation of one-sided boundary layers near discontinuities of the flux function (for example, near $x = 0$ in Figures 7 (c) and (d)). Scheme 2 exhibits smaller numerical viscosity, while Scheme 3 sharply resolves all flux discontinuities. Both Schemes 2 and 3 sharply resolve the solution near $x_{\mathrm{D}} = -1$. Let us comment that the superiority of Scheme 3 is in part balanced by the slightly increased effort needed to evaluate the flux functions h^2 and h^3, which need to be calculated anew (by a discussion of extrema) for each value of the control variables q_{R}, q_{F}, q_{D} and u_{F}.

$J = 1/\Delta x$	$t = 0.5$		$t = 2$	
	approx. L^1 error	conv. rate	approx. L^1 error	conv. rate
	Scheme 1			
20	1.715e-2		6.214e-2	
40	1.195e-2	0.522	4.418e-2	0.492
80	8.363e-3	0.515	2.616e-2	0.756
160	5.610e-3	0.576	1.510e-2	0.793
320	3.571e-3	0.652	8.573e-3	0.817
	Scheme 2			
20	7.785e-3		8.310e-3	
40	5.285e-3	0.559	4.332e-3	0.940
80	3.422e-3	0.627	2.221e-3	0.963
160	2.081e-3	0.718	1.107e-3	1.005
320	1.174e-3	0.826	5.171e-4	1.098
	Scheme 3			
20	8.067e-3		7.033e-3	
40	5.045e-3	0.677	3.694e-3	0.929
80	3.003e-3	0.749	1.903e-3	0.957
160	1.674e-3	0.843	9.476e-4	1.006
320	8.487e-4	0.980	4.379e-4	1.114

TABLE 3. Approximate L^1 errors for Case 1.

ACKNOWLEDGEMENTS

RB acknowledges support by Sonderforschungsbereich 404 at the University of Stuttgart, DAAD/Conicyt Alechile programme, Fondecyt project 1050728 and Fondap in Applied Mathematics. AG acknowledges support by MECESUP project UCO0406. The research of KHK is supported by an Outstanding Young Investigators Award (OYIA) from the Research Council of Norway. Portions of this research were conducted while RB and JDT visited Centre of Mathematics for Applications (CMA) at the University of Oslo, and they are grateful to OYIA for financial support.

REFERENCES

[1] ADIMURTHI & VEERAPPA GOWDA, G.D. (2002) Conservation law with discontinuous flux. *J. Math. Kyoto Univ.*, **42**, 27–70.

[2] AMADORI, D., GOSSE, L. & GUERRA G. (2004) Godunov-type approximation for a general resonant balance law with large data. *J. Differential Equations*, **198**, 233–274.

[3] AUDUSSE, E. & PERTHAME, B. (2005) Uniqueness for a scalar conservation law with discontinuous flux via adapted entropies. *Proc. Royal Soc. Edinburgh Sect. A*, **135**, 253–265.

[4] BERRES, S., BÜRGER, R., KARLSEN, K.H. & TORY, E.M. (2003) Strongly degenerate parabolic-hyperbolic systems modeling polydisperse sedimentation with compression. *SIAM J. Appl. Math.*, **64**, 41–80.

[5] BERRES, S., BÜRGER, R. & KARLSEN, K.H. (2004) Central schemes and systems of conservation laws with discontinuous coefficients modeling gravity separation of polydisperse suspensions. *J. Comp. Appl. Math.*, **164-165**, 53–80.

(a) Case 5, $t = 1$, $\Delta x = 1/40$

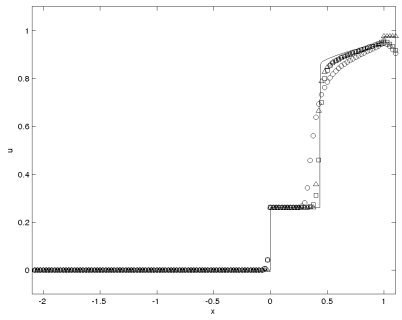

(b) Case 5, $t = 1$, $\Delta x = 1/80$

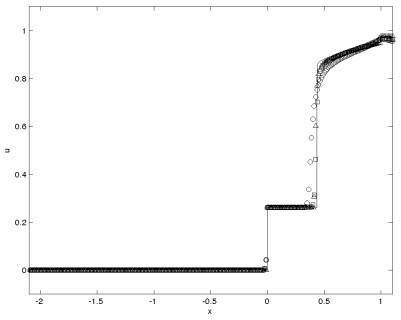

(c) Case 5, $t = 2$, $\Delta x = 1/40$

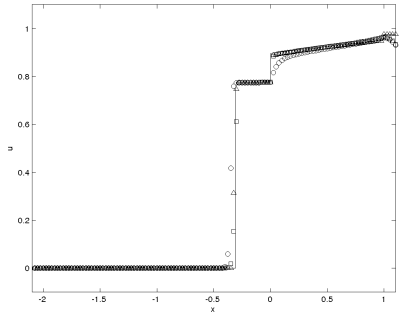

(d) Case 5, $t = 2$, $\Delta x = 1/80$

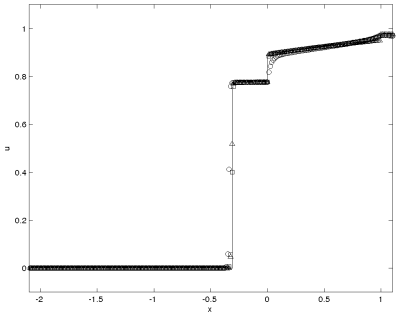

(e) Case 5, $t = 4$, $\Delta x = 1/40$

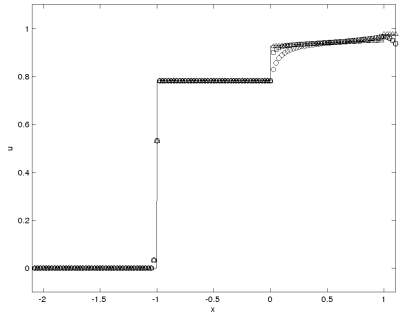

(f) Case 5, $t = 4$, $\Delta x = 1/80$

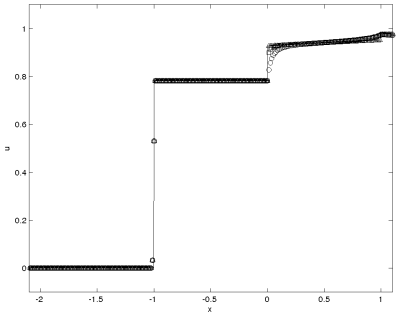

FIGURE 6. Comparison of Scheme 1 (○), Scheme 2 (□) and Scheme 3 (△) applied to Case 5. The solid line is a reference solution with $\Delta x = 1/1600$.

[6] BÜRGER, R. & KARLSEN, K.H. (2003) On a diffusively corrected kinematic-wave traffic flow model with changing road surface conditions. *Math. Models Methods Appl. Sci.*, **13**, 1767–1799.

[7] BÜRGER, R., KARLSEN, K.H., KLINGENBERG, C. & RISEBRO, N.H. (2003) A front tracking approach to a model of continuous sedimentation in ideal clarifier-thickener units. *Nonlin. Anal. Real World Appl.*, **4**, 457–481.

$J = 1/\Delta x$	$t = 1$		$t = 2$		$t = 4$	
	approx. L^1 error	conv. rate	approx. L^1 error	conv. rate	approx. L^1 error	conv. rate
	Scheme 1					
20	1.139e-1		9.123e-2		7.228e-2	
40	6.561e-2	0.796	4.836e-2	0.916	2.739e-2	1.400
80	4.000e-2	0.714	3.178e-2	0.605	1.488e-2	0.880
160	2.587e-2	0.628	2.123e-2	0.582	8.269e-2	0.848
320	1.665e-2	0.636	1.383e-2	0.619	4.521e-3	0.871
	Scheme 2					
20	7.118e-2		6.616e-2		5.614e-2	
40	2.876e-2	1.308	2.201e-2	1.588	1.856e-2	1.597
80	1.268e-2	1.182	1.106e-2	0.994	1.001e-2	0.891
160	7.428e-3	0.771	5.740e-3	0.946	5.577e-3	0.844
320	4.713e-3	0.656	4.111e-3	0.482	3.025e-3	0.882
	Scheme 3					
20	3.483e-2		3.151e-2		2.466e-2	
40	1.990e-2	0.808	1.753e-2	0.846	1.241e-2	0.991
80	1.101e-2	0.854	9.637e-3	0.863	6.164e-3	1.009
160	6.118e-3	0.847	3.984e-3	1.274	2.979e-3	1.049
320	3.128e-3	0.968	1.906e-3	1.064	1.352e-3	1.140

TABLE 4. Approximate L^1 errors for Case 5.

[8] BÜRGER, R., KARLSEN, K.H., MISHRA, S. & TOWERS, J.D. (2005) On conservation laws with discontinuous flux. In: Y. Wang & K. Hutter (Eds.), Trends in Applications of Mathematics to Mechanics, Shaker Verlag, Aachen, 75–84.

[9] BÜRGER, R., KARLSEN, K.H., RISEBRO, N.H. & TOWERS, J.D. (2004) Numerical methods for the simulation of continuous sedimentation in ideal clarifier-thickener units. *Int. J. Mineral Process.*, **73**, 209–228.

[10] BÜRGER, R., KARLSEN, K.H., RISEBRO, N.H. & TOWERS, J.D. (2004) Well-posedness in BV_t and convergence of a difference scheme for continuous sedimentation in ideal clarifier-thickener units. *Numer. Math.*, **97**, 25–65.

[11] BÜRGER, R., KARLSEN, K.H. & TOWERS, J.D. (2005) Closed-form and finite difference solutions to a population balance model of grinding mills. *J. Eng. Math.*, **51**, 165–195.

[12] BÜRGER, R., KARLSEN, K.H. & TOWERS, J.D. (2005) A model of continuous sedimentation of flocculated suspensions in clarifier-thickener units. *SIAM J. Appl. Math.*, **65**, 882–940.

[13] BÜRGER, R., KARLSEN, K.H. & TOWERS, J.D. (2005) Mathematical model and numerical simulation of the dynamics of flocculated suspensions in clarifier-thickeners. *Chem. Eng. J.*, **111**, 119–134.

[14] BÜRGER, R., KARLSEN, K.H. & TOWERS, J.D. A discontinuous viscosity scheme for conservation laws with a spatially discontinuous coefficient. To appear.

[15] BUSTOS, M.C., CONCHA, F., BÜRGER, R. & TORY, E.M. (1999) Sedimentation and Thickening. Kluwer Academic Publishers, Dordrecht, The Netherlands.

[16] ČANIĆ, S. & MIRKOVIĆ, D. (2001) A hyperbolic system of conservation laws in modeling endovascular treatment of abdominal aortic aneurysm. In: Freistühler, H. and Warnecke, G. (eds.), Hyperbolic Problems: Theory, Numerics, Applications. Eighth International Conference in Magdeburg, February/March 2000, Volume I. International Series of Numerical Mathematics **140**, Birkhäuser Verlag, Basel, 227–236.

[17] CRANDALL, M.G. & MAJDA, A. (1980) Monotone difference approximations for scalar conservation laws. *Math. Comp.*, **34**, 1–21.

(a) Case 7, $t = 0.3$, $\Delta x = 1/40$ (b) Case 7, $t = 0.3$, $\Delta x = 1/80$

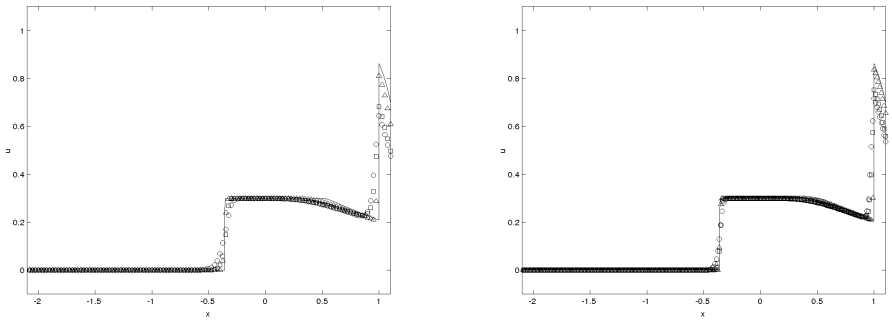

(c) Case 7, $t = 10$, $\Delta x = 1/40$ (d) Case 7, $t = 10$, $\Delta x = 1/80$

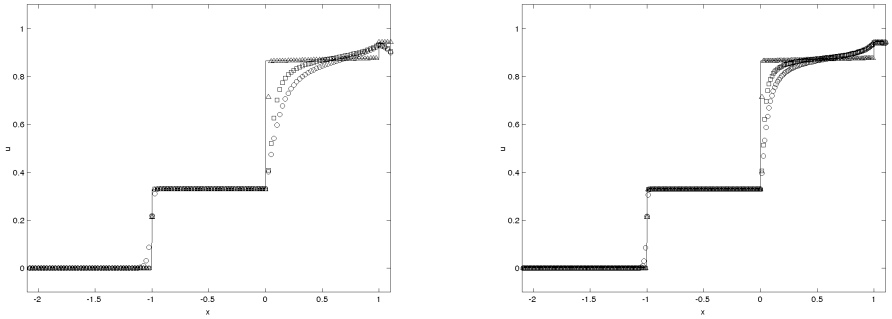

FIGURE 7. Comparison of Scheme 1 (○), Scheme 2 (□) and Scheme 3 (△) applied to Case 7. The solid line is a reference solution with $\Delta x = 1/1600$.

[18] DIEHL, S. (1995) On scalar conservation laws with point source and discontinuous flux function. *SIAM J. Math. Anal.*, **26**, 1425–1451.

[19] DIEHL, S. (1996) A conservation law with point source and discontinuous flux function modelling continuous sedimentation. *SIAM J. Appl. Math.*, **56**, 388–419.

[20] DIEHL, S. (1996) Scalar conservation laws with discontinuous flux function: I. The viscous profile condition. *Commun. Math. Phys.*, **176**, 23–44.

[21] DIEHL, S. (1997) Dynamic and steady-state behaviour of continuous sedimentation. *SIAM J. Appl. Math.*, **57**, 991–1018.

[22] DIEHL, S. (2000) On boundary conditions and solutions for ideal clarifier-thickener units. *Chem. Eng. J.*, **80**, 119–133.

[23] DIEHL, S. (2001) Operating charts for continuous sedimentation I: Control of steady states. *J. Eng. Math.*, **41**, 117–144.

[24] DIEHL, S. & WALLIN, N.-O. (1996) Scalar conservation laws with discontinuous flux function: II. On the stability of the viscous profiles. *Commun. Math. Phys.*, **176**, 45–71.

[25] ENGQUIST, B. & OSHER, S. (1981) One-sided difference approximations for nonlinear conservation laws. *Math. Comp.*, **36**, 321–351.

[26] GALVIN, K.P., CALLEN, A., ZHOU, J. & DOROODCHI, E. (2005) Performance of the reflux classifier for gravity separation at full scale. *Minerals Eng.*, **18**, 19–24.

[27] GALVIN, K.P., DOROODCHI, E., CALLEN, A.M., LAMBERT, N. & PRATTEN, S.J. (2002) Pilot plant trial of the reflux classifier. *Minerals Eng.*, **15**, 19–25.

[28] GALVIN, K.P. & NGUYENTRANLAM, G. (2002) Influence of parallel plates in a liquid fluidized bed system. *Chem. Eng. Sci.*, **57**, 1231–1234.

$J = 1/\Delta x$	$t = 0.3$		$t = 10$	
	approx. L^1 error	conv. rate	approx. L^1 error	conv. rate
	Scheme 1			
20	9.406e-2		1.946e-1	
40	6.394e-2	0.557	1.069e-1	0.864
80	4.255e-2	0.588	6.332e-2	0.756
160	2.685e-2	0.664	3.694e-2	0.778
320	1.609e-2	0.739	2.084e-2	0.826
	Scheme 2			
20	7.619e-2		1.365e-1	
40	5.023e-2	0.601	7.423e-2	0.879
80	3.176e-2	0.661	4.303e-2	0.787
160	1.888e-2	0.751	2.465e-2	0.804
320	1.069e-2	0.821	1.358e-2	0.860
	Scheme 3			
20	3.092e-2		4.109e-2	
40	1.738e-2	0.831	2.041e-2	1.010
80	9.185e-3	0.920	1.000e-2	1.029
160	4.420e-3	1.055	4.766e-3	1.069
320	2.134e-3	1.051	2.131e-3	1.161

TABLE 5. Approximate L^1 errors for Case 7.

[29] GIMSE, T. (1993) Conservation laws with discontinuous flux functions. *SIAM J. Math. Anal.*, **24**, 279–289.

[30] GIMSE, T. & Risebro, N.H. (1992) Solution of the Cauchy problem for a conservation law with a discontinuous flux function. *SIAM J. Math. Anal.*, **23**, 635–648.

[31] HARTEN, A. (1983) High resolution schemes for hyperbolic conservation laws. *J. Comp. Phys.*, **49**, 357–393.

[32] KAASSCHIETER, E.F. (1999) Solving the Buckley-Leverett equation with gravity in a heterogeneous porous medium. *Comput. Geosci.*, **3**, 23–48.

[33] KARLSEN, K.H., KLINGENBERG, C. & RISEBRO, N.H. (2003) A relaxation scheme for conservation laws with a discontinuous coefficient. *Math. Comp.* **73**, 1235–1259.

[34] KARLSEN, K.H., RISEBRO, N.H. & TOWERS, J.D. (2003) L^1 stability for entropy solutions of nonlinear degenerate parabolic convection-diffusion equations with discontinuous coefficients. *Skr. K. Nor. Vid. Selsk.*, 49 pp.

[35] KARLSEN, K.H. & TOWERS, J.D. (2004) Convergence of the Lax-Friedrichs scheme and stability for conservation laws with a discontinuous space-time dependent flux. *Chin. Ann. Math.*, **25B**, 287–318.

[36] KLAUSEN, R.A. & RISEBRO, N.H. (1999) Stability of conservation laws with discontinuous coefficients. *J. Diff, Eqns.*, **157**, 41–60.

[37] KLINGENBERG, C. & RISEBRO, N.H. (1995) Convex conservation laws with discontinuous coefficients. *Comm. PDE*, **20**, 1959–1990.

[38] KRUŽKOV, S.N. (1970) First order quasilinear equations in several independent variables. *Math. USSR Sb.*, **10**, 217–243.

[39] KYNCH, G.J. (1952) A theory of sedimentation. *Trans. Faraday Soc.*, **48**, 166–176.

[40] MISHRA, S. (2005) Convergence of upwind finite difference schemes for a scalar conservation law with indefinite discontinuities in the flux function. *SIAM J. Numer. Anal.*, **43**, 559–577.

[41] MOCHON, S. (1987) An analysis of the traffic on highways with changing road surface conditions. *Math. Modelling*, **9**, 1–11.

[42] Nasr-El-Din, H., Masliyah, J.H. & Nandakumar, K. (1990) Continuous gravity separation of concentrated bidisperse suspensions in a vertical column. *Chem. Eng. Sci.*, **45**, 849–857.
[43] Nasr-El-Din, H., Masliyah, J.H. & Nandakumar, K. (1999) Continuous separation of suspensions containing light and heavy particle species. *Canad. J. Chem. Eng.*, **77**, 1003–1012.
[44] Nasr-El-Din, H., Masliyah, J.H., Nandakumar, K. & Law, D.H.-S. (1988) Continuous gravity separation of a bidisperse suspension in a vertical column. *Chem. Eng. Sci.*, **43**, 3225–3234.
[45] Nguyentranlam, G. & Galvin, K.P. (2001) Particle classification in the reflux classifier. *Minerals Eng.*, **14**, 1081–1091.
[46] Ostrov, D. (2002) Solutions of Hamilton-Jacobi equations and scalar conservation laws with discontinuous space-time dependence, *J. Diff. Eqns.*, **182**, 51–77.
[47] Richardson, J.F. & Zaki, W.N. (1954) Sedimentation and fluidization: Part I. *Trans. Instn. Chem. Engrs. (London)*, **32**, 35–53.
[48] Ross, D.S. (1988) Two new moving boundary problems for scalar conservation laws. *Comm. Pure Appl. Math.*, **41**, 725–737.
[49] Seguin, N. & Vovelle, J. (2003) Analysis and approximation of a scalar conservation law with a flux function with discontinuous coefficients. *Math. Models Meth. Appl. Sci.*, **13**, 221–257.
[50] Spannenberg, A., Galvin, K., Raven, J. & Scarboro, M. (1996) Continuous differential sedimentation of a binary suspension. *Chem. Eng. in Australia*, **21**, 7–11.
[51] Towers, J.D. (2000) Convergence of a difference scheme for conservation laws with a discontinuous flux. *SIAM J. Numer. Anal.*, **38**, 681–698.
[52] Towers, J.D. (2001) A difference scheme for conservation laws with a discontinuous flux: The nonconvex case. *SIAM J. Numer. Anal.*, **39**, 1197–1218.
[53] Van Duijn, C.J., De Neef, M.J. & Molenaar, J. (1995) Effects of capillary forces on immiscible two-phase flow in strongly hetereogeneous porous media. *Transp. Porous Media*, **21**, 71–93.